
Týr-the-Pruner: Structural Pruning LLMs via Global Sparsity Distribution Optimization

Guanchen Li, Yixing Xu, Zeping Li, Ji Liu, Xuanwu Yin, Dong Li, Emad Barsoum

Advanced Micro Devices, Inc. (AMD)

{guanchen, yixing.xu, zeping.li, ji.liu, xuanwu.yin, d.li, emad.barsoum}@amd.com

Abstract

Structural pruning enhances hardware-agnostic inference efficiency for large language models (LLMs) yet often fails to maintain comparable performance. Local pruning performs efficient layer-by-layer compression but ignores global topology. Although global pruning aims to identify an optimal sparse model, intuitive methods typically adopt a two-stage paradigm that first evaluates substructure saliency and then applies global pruning, which ignores inter-structure dependencies and fails to achieve end-to-end optimization. To address these limitations, we propose **Týr-the-Pruner**, an efficient end-to-end search-based global structural pruning framework. This framework constructs a supernet by repeatedly applying local pruning across a range of sparsity ratios to each layer in an LLM, with the core goal of determining the optimal sparsity distribution under a target overall sparsity ratio. Concretely, we introduce an effective local pruning and an expectation error accumulation approach to improve supernet construction. Furthermore, we employ an iterative prune-and-search strategy with coarse-to-fine sparsity granularity to ensure efficient search convergence. Experimental results show that Týr-the-Pruner achieves state-of-the-art structural pruning, retaining **97%** of the dense model’s performance while removing a challenging **50%** of Llama-3.1-70B’s parameters. Code will be available at <https://github.com/AMD-AGI/Tyr-the-Pruner>.

1 Introduction

Large language models (LLMs) have significantly advanced natural language processing, achieving exceptional performance in tasks such as text understanding, generation, and reasoning [51, 7, 3]. However, the computational and storage resources required for model deployment incur high costs and environmental impacts, limiting their accessibility in resource-constrained scenarios. Model compression techniques, such as quantization [21, 10], pruning [9, 23], and low-rank decomposition [43], are essential for reducing LLM size and computational demands. This paper focuses on structural pruning, which enhances inference efficiency in a hardware-agnostic manner.

Existing structural pruning methods for LLMs are typically classified into local and global techniques. Local pruning methods [17, 26], which prune layers individually, enable efficient compression of hundred-billion-scale LLMs on a single GPU via offload approaches. However, they overlook global dependencies in model topology and restrict the sparsity to be uniform across layers. Global pruning methods [23, 18, 1] alleviate local constraints, facilitating sparsity allocation and the potential for optimal pruning. However, many existing methods estimate the saliency of local substructures and prune them accordingly via global ranking, ignoring inter-structure dependencies and hindering end-to-end optimization. Such methods may also suffer from the inefficiency of backpropagation-based saliency estimation and overfitting when calibration data is limited. Therefore, a question arises:

How to achieve efficient global structural pruning with end-to-end optimization?

To address this challenge, we propose **Týr-the-Pruner**, an efficient search-based global pruning framework with end-to-end optimization. Our framework constructs a supernet by applying local pruning to each layer, producing pruned copies with different sparsity ratios. The objective is to identify an optimal subnet that satisfies the target overall sparsity ratio within the supernet by determining the optimal sparsity distribution across layers. We use evolutionary search [22] to solve this optimization problem. To construct reliable supernets and perform effective and efficient search, we make the following contributions:

- **To improve supernet construction**, we propose an effective local pruning approach for attention heads and feed-forward networks (FFN), using Taylor expansion-based first- and second-order optimization information to identify redundant structures and adjust remaining weights. Pruning and weight adjustments are applied progressively and finely to preserve accuracy. Additionally, we introduce an expectation error accumulation approach to address the challenge of unclear error propagation caused by the multiple pruned copies within the supernet. This approach ensures balanced mutual awareness across sparse structures during supernet construction.
- **To enhance the efficacy and efficiency of subnet search**, we employ a tailored distillation-inspired metric as the optimization objective to guide the search process, aiming to preserve the subnet’s generative capability. In general, Týr-the-Pruner is formed as an iterative prune-and-search framework that refines sparsity allocation for each layer with reduced search space and fast convergence. Each iteration prunes and constructs a supernet across a specific range of sparsity ratios, coupled with a sparsity-shift-driven evolutionary search, where random sparsity shifts between layers generate parent candidates, and the best-performing ones are filtered as offspring. The sparsity interval is refined after each iteration.

By making these contributions, Týr-the-Pruner achieves end-to-end global pruning with strong efficacy and efficiency. Notably, the proposed framework only requires 4M tokens for calibration and search. Experimental results demonstrate that Týr-the-Pruner surpasses state-of-the-art pruning methods. For example, Týr-the-Pruner outperforms the SOTA method FLAP, achieving 3.45 lower perplexity in language comprehension and 10.26% higher average downstream accuracy when pruning 37.5% of the parameters of Llama-3.1-8B. Moreover, it maintains 97% performance with 50% pruning on Llama-3.1-70B, a sparsity ratio that is considered aggressive for existing methods.

2 Method

This section presents Týr-the-Pruner, a novel structural pruning framework for large language models (cf. Section 2.1 for preliminaries), as illustrated in Figure 1. This framework **(1) constructs a supernet** by applying local pruning across various sparsity ratios to each model layer, aiming to **(2) search the optimal sparsity distribution** under a target overall sparsity ratio. Specifically, we propose an effective local pruning approach (cf. Section 2.2) and an expectation error accumulation approach (cf. Section 2.3) to enhance supernet construction. An iterative prune-and-search strategy with coarse-to-fine sparsity granularity (cf. Section 2.4) ensures efficient search convergence.

2.1 Preliminaries

Large language models typically use the Transformer decoder architecture [40], as shown in Figure 1(a). Each Transformer layer consists of two key components: the multi-head self-attention (MHA) and the feed-forward network (FFN), followed by a residual connection and layer normalization. Given the input $\mathbf{X}_{\ell-1}$ to the ℓ -th layer, the output \mathbf{X}_ℓ can be expressed as:

$$\begin{aligned} \mathbf{X} &= \text{LayerNorm}(\mathbf{X}_{\ell-1} + \text{MHA}(\mathbf{X}_{\ell-1})), \\ \mathbf{X}_\ell &= \text{LayerNorm}(\mathbf{X} + \text{FFN}(\mathbf{X})). \end{aligned} \tag{1}$$

The MHA mechanism captures dependencies across different positions in the input sequence with multiple attention heads, each with its query (\mathbf{W}_q), key (\mathbf{W}_k), value (\mathbf{W}_v), and out (\mathbf{W}_o) linear transformations. Modern LLMs typically employ a SwiGLU-based FFN [34], consisting of gate (\mathbf{W}_{gate}), up (\mathbf{W}_{up}), and down (\mathbf{W}_{down}) linear transformations, with activation after the gate. This structure aids in extracting non-linear representations.

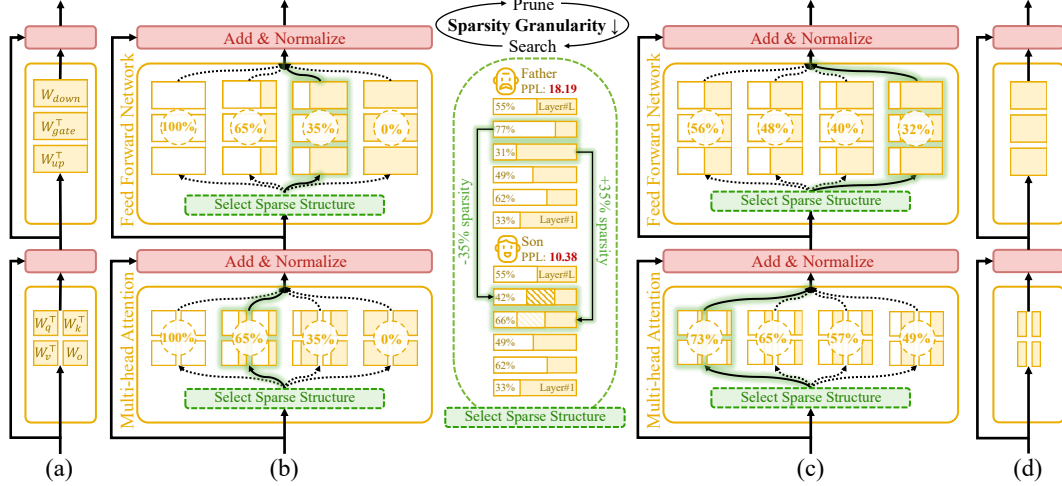


Figure 1: **An overview for Týr-the-Pruner.** Large language models (a) will be effectively locally pruned across multiple sparsity ratios and constructed into a supernet (b). An iterative prune-and-search strategy will be used to select the optimal sparse structure for each layer while maintaining a target overall sparsity ratio: pruning and sparsity-shift-driven evolutionary search are implemented iteratively with a coarse-to-fine sparsity interval granularity (c). Ultimately, the post-pruned LLM with the optimal sparsity distribution (d) is obtained.

Structural pruning for LLMs can be applied across four key dimensions: (1) attention heads, (2) FFN intermediate neurons, (3) embedding dimension size, and (4) model depth. It can be isotropic (uniform sparsity across layers) or non-isotropic (layer-specific sparsity). This paper focuses on pruning attention heads and FFN intermediate neurons with non-uniform sparsity: pruning functionally independent heads and neurons allows for controllable accuracy loss, while layer-specific sparsity further enhances pruning by tailoring compression to each layer’s characteristics.

2.2 Effective Local Pruning

Redundant structure identification and weight adjustment. When pruning is scoped to the local level, one can determine the pruning outcome by eliminating the redundant input channels of each o_proj and down_proj modules, with a consistent sparsity across layers. Assuming the weight of a layer is $\mathbf{W} \in \mathbb{R}^{d_{\text{in}} \times d_{\text{out}}}$ and its input activation is $\mathbf{X} \in \mathbb{R}^{d_{\text{N}} \times d_{\text{in}}}$, the pruned weight $\widehat{\mathbf{W}}$ satisfies the sparsity constraint C . The corresponding optimization objective is expressed as:

$$\operatorname{argmin}_{\widehat{\mathbf{W}}} \|\mathbf{X}\mathbf{W} - \mathbf{X}\widehat{\mathbf{W}}\|_2^2 \quad \text{s.t.} \quad \mathcal{C}(\widehat{\mathbf{W}}) = C. \quad (2)$$

The pruning process can be viewed as a perturbation applied to the weights: $\widehat{\mathbf{W}} = \mathbf{W} - \delta\mathbf{W}$. Therefore, the error function is given by $E = \|\mathbf{X}\mathbf{W} - \mathbf{X}\widehat{\mathbf{W}}\|_2^2 = \|\mathbf{X}\delta\mathbf{W}\|_2^2$, which can be approximated by a Taylor series expansion around \mathbf{W} and whose local fluctuations can be defined as:

$$\delta E = \underbrace{\left(\frac{\partial E}{\partial \mathbf{W}} \right)^\top \delta \mathbf{W}}_{\mathbf{G}^\top \approx 0} + \frac{1}{2} \delta \mathbf{W}^\top \underbrace{\frac{\partial^2 E}{\partial \mathbf{W}^2} \delta \mathbf{W}}_{\mathbf{H} \neq 0} + \underbrace{O(\|\delta \mathbf{W}\|^3)}_{\approx 0}. \quad (3)$$

δE reflects the effect of $\delta\mathbf{W}$ on the pruning error, which we aim to minimize. The first-order gradient \mathbf{G} cannot be neglected, as the calibration samples are inevitably misaligned with the proprietary closed-source pre-training data. The Hessian matrix \mathbf{H} helps to identify pruning-sensitive weights from a curvature perspective. Considering the sparsity constraint ($\delta \mathbf{W}_{p,:} = \mathbf{W}_{p,:}$: the p -th input channel of \mathbf{W} is to be pruned), we design the redundant channels and weight adjustment as follows:

$$\mathbf{W}_{p,:} = \operatorname{argmin}_{\mathbf{W}_{p,:}} \left(|\mathbf{G}_{p,:} \mathbf{W}_{p,:}^\top| + \frac{\|\mathbf{W}_{p,:}\|_2^2}{2 [\mathbf{H}^{-1}]_{p,p}} \right), \quad \delta \mathbf{W}_{\sim p,:} = -\mathbf{H}_{\sim p, \sim p}^{-1} \mathbf{G}_{\sim p,:}. \quad (4)$$

$\mathbf{H} = \mathbf{X}^\top \mathbf{X}$ and $\mathbf{G} = \mathbf{H}\mathbf{W}$ (analytic solutions computed without backpropagation, efficient) are used as estimates of the local optimization information. The channel p with the least error impact is identified and pruned, while $\delta \mathbf{W}$ adjusts the remaining weights to compensate for pruning errors ($\sim p$ represents other channels that have not been pruned).

Pruning heads and neurons. In our framework, feed-forward network neurons are pruned based on individual channel saliency computed from the `down_proj` layer, where each channel acts as the atomic unit for ranking and removal. For multi-head self-attention, saliency is first computed per output channel of the `o_proj` layer, then aggregated (averaged) across channels belonging to the same head, which is treated as the atomic unit for pruning.

Progressively pruning and weight adjustment. We adopt progressive pruning with an appropriately fine granularity: finer granularity enables unpruned weights to gradually and uniformly compensate for pruning losses in small increments while enabling precise and dynamic redundant channel identification. Reducing granularity does not significantly complicate pruning, as the key intermediate variable \mathbf{H}^{-1} can be rapidly adjusted to account for partial channel pruning in $O(d_{\text{in}}^2)$ complexity [8].

Detailed analysis can be found in Section A.1.

2.3 Prune-to-supernet across Multiple Sparsity Ratios

As illustrated in Figure 1(b), a supernet will be constructed by repeatedly applying local pruning across a range of sparsity ratios to each LLM layer, producing pruned copies with varying sparsity ratios. However, this introduces challenges in error accumulation across layers. Error accumulation introduces an additional forward pass of the post-pruned layer, using its output activation as input for the next layer. The change in the input directly affects the optimization of the subsequent layer. In the example shown in Figure 2, pruning half of Llama-3.1-8B’s parameters using the local pruning approach with error accumulation results in significantly lower language comprehension perplexity than pruning without it. This performance gap highlights the critical role of error accumulation: it enables deeper layer pruning to be aware of shallower layer pruning.

The existence of multiple sparse structures complicates error accumulation, making it unclear which pathway to prioritize. To address this issue, we propose an *expectation error accumulation* approach to enable balanced mutual awareness among the sparse structures in the supernet. Let the output activation of the e -th sparse structure with sparsity S_e in layer ℓ be $\mathbf{X}_{\ell+1,e}$. We define the expectation output activation $\mathbf{X}_{\ell+1}$ for this layer as:

$$\mathbf{X}_{\ell+1} = \sum_{e=1}^E \frac{1 - S_e}{\sum_{e=1}^E (1 - S_e)} \mathbf{X}_{\ell+1,e}. \quad (5)$$

A higher scaling factor is assigned to low sparsity weights because their output activations are more stable and reliable. By enabling expectation error accumulation and applying the local pruning approach, we can prune Llama-3.1-8B to create nine sparse structures in each layer, with 12.5% as the sparsity interval (covers complete pruning and abandoned pruning). The post-pruned model achieves a language comprehension perplexity of 66.38 on the WikiText-2 task, with manually picking the 50% sparse structure as an example. This result is close to the ideal perplexity of 58.09 achieved under full error accumulation and significantly better than the 208.92 perplexity from random error accumulation and 538.23 perplexity with abandoned error accumulation.

2.4 Týr-the-Pruner

By introducing effective local pruning and expectation error accumulation approaches, we can construct a supernet to tackle the global sparsity allocation problem. Specifically, we address the following issues to achieve efficient and effective sparsity allocation: (1) defining generalizable criteria for selecting a better sparse structure, (2) achieving an efficient search-based sparse structure selection while maintaining overall sparsity, and (3) handling the contradiction between fine-grained sparsity intervals and the large search space.

Align to dense model behaviors to win. Towards the definition of better sparse structures, we consider that large language models are designed for multi-task generalization. Thus, guiding sparse structure selection on a single task risks overfitting. To mitigate this, we adopt a distillation-inspired metric to measure the similarity between sparse and dense models. A salient similarity indicates that the current sparse structure is better aligned with the dense model, making it more suitable for selection. Specifically, let $\mathbf{h}_\ell^{\text{dense}}$ and $\mathbf{h}_{\ell,e}^{\text{sparse}}$ denote the activations of the dense and e -th sparse (structure) models at layer ℓ , and $\mathbf{z}^{\text{dense}}$ and $\mathbf{z}_{\{e\}}^{\text{sparse}}$ represent the logits of the dense model and selected $\{\{e\} = \{e_\ell\}_{\ell=1}^L\}$ sparse subnet. The optimization objective is formulated as follows:

$$\{\hat{e}\} = \operatorname{argmin}_{\{e\}} \sum_{\ell} \alpha_{\ell} \left\| \mathbf{h}_\ell^{\text{dense}} - \mathbf{h}_{\ell,e}^{\text{sparse}} \right\|_2^2 + \beta \operatorname{KL}(\mathbf{z}^{\text{dense}} \parallel \mathbf{z}_{\{e\}}^{\text{sparse}}). \quad (6)$$

Sparse structure selection via evolutionary search. Evolutionary search can achieve convergence in model architecture optimization [36, 22]. Compared to intuitive router training, evolutionary search requires no additional parameters. It maintains constant overall sparsity by shifting sparsity between sparse structures from different layers, whereas router training relies on penalty terms for suboptimal soft sparsity control. Evolutionary search is efficient, as it allows the just-in-time loading (cf. Section 3.5) of sparse structures and leverages the backpropagation-free feature.

Mutation (stochastic perturbation) in our evolutionary search arises from sparsity shifts across layers (cf. *Select Sparse Structure* in Figure 1). For instance, the sparsity of the ℓ -th layer may decrease by $s\%$, while the ℓ' -th layer increases by $s\%$ (achieved by selecting different sparse structures). In each generation, we randomly generate such a group of sparsity distributions as candidates. Starting from the root generation, the performance of candidates is evaluated, and the best-performing ones are selected to generate new candidates for the next generation. Generations continue to be explored until the optimal sparsity distribution is found.

Iterative prune-to-supernet and evolutionary search. The search space for selecting sparse structures with fine-grained sparsity is enormous. For instance, constructing a supernet with a sparsity interval of 1.5625% would result in 65 sparse structures per MHA/FFN layer. For a 40-layer LLM, this would lead to over 5K sparse structures, creating a 10^{145} -scaled search space. Identifying solutions in this large search space is difficult and costly. To address this challenge, Týr-the-Pruner adopts an iterative prune-and-search strategy that progressively refines sparsity granularity. In each iteration, we (1) prune the model, (2) construct a supernet with a narrower sparsity interval, and (3) perform evolutionary search to locate the optimal sparsity distribution. This coarse-to-fine paradigm improves both search efficiency and accuracy in sparse structure discovery, as illustrated below.

Example: Týr-the-Pruner

Týr-the-Pruner starts by constructing a coarse-grained supernet (e.g., Figure 1(b)) using a 12.5% sparsity interval, where each MHA/FFN layer contains only nine candidate structures. Evolutionary search is then applied to determine the optimal sparsity pattern at this iteration. In the subsequent iteration, a new supernet (e.g., Figure 1(c)) is constructed by halving the sparsity interval to 6.25% and centering it on the current optimum (e.g., 37.5%), yielding nine refined candidates from sparsity 12.5% to 62.5%, followed by evolutionary search to update the optimal sparsity. With the sparsity interval halved at each iteration, Týr-the-Pruner narrows the search space to about 10^{76} per iteration and reaches a 1.5625% sparsity granularity within four iterations. This coarse-to-fine refinement enhances both efficiency and accuracy in identifying the optimal fine-grained sparsity for final model compression (e.g., Figure 1(d)).

The algorithmic procedures for local pruning, supernet construction, evolutionary search, and the overall Týr-the-Pruner framework are detailed in Algorithms 1 to 4 of Section A.2.

Table 1: **Post pruning performance comparison of different methods.** Language comprehension perplexity is validated on the Wikitext2 test set with a sequence length of 4096, where a lower value reflects better performance. Downstream accuracy (%), higher is better) is averaged across ARC-Easy, ARC-Challenge, BoolQ, HellaSwag, OpenbookQA, RTE, WinoGrande, and MMLU, with MMLU using a 5-shot benchmark and others a 0-shot benchmark. The best results are shown in **bold**.

Sparsity	Method	Perplexity on Wikitext2 ↓						Average Downstream Accuracy (%) ↑							
		Llama-2		Llama-3.x		Mistral		Llama-2		Llama-3.x		Mistral			
		7B	13B	2-3B	0-8B	1-8B	7B-v0.3	Nemo	7B	13B	2-3B	0-8B	1-8B		
0%	N/A	5.12	4.57	7.29	5.76	5.84	4.95	5.35	57.96	62.05	57.01	64.08	64.77	63.72	66.24
12.5%	ShortGPT	8.86	5.67	12.42	13.90	13.14	7.58	7.72	53.27	59.16	53.13	57.75	58.50	59.49	59.46
	LaCO+	7.52	5.69	12.25	10.12	9.98	7.46	7.95	53.23	57.26	52.46	59.41	60.36	58.67	59.96
	SliceGPT	8.25	7.19	18.71	20.46	22.10	7.00	9.74	55.89	59.70	51.64	57.55	56.82	59.67	53.27
	Wanda-sp	6.24	6.09	182.24	86.91	18.46	6.86	7.27	55.40	57.41	38.02	33.95	47.89	59.44	56.82
	LLM-Pruner	6.11	5.17	11.14	8.24	8.26	6.17	6.79	53.38	59.78	46.98	53.96	54.04	55.26	58.23
	ZipLM	5.86	5.21	11.32	10.37	9.30	5.84	7.62	55.85	61.91	51.37	57.55	57.54	62.46	60.24
	OSSCAR	5.94	5.21	11.11	10.15	9.87	5.75	7.04	55.29	61.94	52.23	57.19	58.53	62.06	53.89
	FLAP	6.11	5.75	10.25	8.34	8.07	6.18	7.68	54.63	57.55	47.74	55.72	56.66	59.51	57.67
25%	Týr-the-Pruner	5.84	5.03	9.16	7.39	7.41	5.61	6.31	56.98	62.66	54.78	62.01	63.02	63.05	64.15
	ShortGPT	23.41	17.94	1464.20	4836.41	3418.83	35.20	124.20	46.68	51.86	41.25	38.12	38.62	51.07	51.68
	LaCO+	18.84	9.00	128.77	124.86	137.17	22.91	20.79	45.47	52.77	46.26	48.58	49.80	51.84	53.65
	SliceGPT	16.84	12.50	45.44	47.73	55.43	12.08	19.37	51.40	58.04	45.87	50.01	48.49	52.26	46.27
	Wanda-sp	9.21	19.92	94.12	48.95	962.72	17.83	15.34	49.92	38.17	33.93	34.53	32.40	49.13	41.30
	LLM-Pruner	11.56	7.11	25.14	18.65	19.35	10.24	11.81	44.09	49.56	39.55	42.36	40.88	46.32	45.26
	ZipLM	7.49	6.65	43.50	28.74	52.69	7.39	9.91	52.59	60.50	41.61	38.72	39.20	58.05	45.59
	OSSCAR	7.46	9.19	122.63	17.40	17.03	7.16	9.57	51.99	59.55	33.29	44.27	42.19	55.94	45.95
37.5%	FLAP	8.31	7.50	15.64	12.65	12.30	8.01	13.59	49.36	54.37	44.01	47.41	49.20	52.64	48.83
	Týr-the-Pruner	7.51	5.79	12.53	13.14	10.38	7.08	7.87	54.64	61.16	51.72	58.50	58.66	60.22	60.61
	ShortGPT	70.96	52.24	554.88	5.1E+04	9.3E+04	2347.69	864.38	43.66	43.13	41.28	39.16	38.97	35.80	42.52
	LaCO+	87.77	96.00	494.07	1645.83	1377.02	429.78	462.92	41.55	47.60	40.24	38.89	38.85	40.44	42.88
	SliceGPT	35.10	26.22	98.41	176.81	237.50	27.68	38.46	43.80	51.83	37.40	39.96	38.97	43.30	39.55
	Wanda-sp	19.97	34.70	344.17	2422.78	3627.00	31.85	74.87	40.45	35.69	33.08	30.59	32.56	38.13	33.59
	LLM-Pruner	37.75	14.96	161.10	87.93	70.93	24.90	32.10	35.96	40.36	33.26	32.40	32.53	37.94	37.42
	ZipLM	12.13	13.01	283.53	50.36	125.98	14.01	15.53	47.53	51.89	33.35	34.77	36.55	48.90	44.86
50%	OSSCAR	11.28	12.74	182.00	27.69	28.87	10.43	16.00	47.42	51.74	32.76	40.81	39.87	48.91	45.81
	FLAP	12.41	11.33	26.05	22.61	21.54	11.81	27.01	43.51	48.54	39.28	41.51	43.07	44.90	45.57
	Týr-the-Pruner	10.29	7.17	27.88	21.64	18.09	10.25	11.47	52.21	58.67	46.11	53.66	53.46	52.34	54.63
	ShortGPT	226.40	187.23	2313.30	1473.71	1678.15	5532.76	6804.52	36.99	39.47	34.09	37.51	36.52	35.05	38.00
	LaCO+	256.71	1129.00	6019.01	2.1E+04	5.4E+04	6019.01	5.9E+04	34.89	41.79	33.96	35.21	33.28	33.93	33.25
	SliceGPT	65.34	50.66	205.09	384.04	353.21	54.66	69.15	39.43	43.84	33.52	34.55	34.32	36.17	34.95
	Wanda-sp	122.28	47.89	262.92	187.41	188.47	91.34	293.59	32.26	35.82	32.29	33.86	32.39	33.59	32.27
	LLM-Pruner	117.40	53.96	473.50	302.15	288.32	74.04	469.93	31.70	35.17	30.97	31.63	31.58	32.64	32.89
	ZipLM	32.91	24.70	356.02	102.76	366.34	24.18	24.96	32.60	42.66	32.51	33.14	34.45	39.93	38.42
	OSSCAR	28.41	44.17	320.14	80.90	198.87	29.58	23.14	39.46	40.40	33.85	32.58	34.16	40.95	37.99
	FLAP	25.49	16.89	272.98	82.12	134.28	34.81	79.46	39.84	44.04	33.29	38.68	36.59	40.57	39.34
	Týr-the-Pruner	16.17	9.59	29.84	38.59	30.89	15.53	16.85	47.41	54.58	41.41	47.41	47.79	46.21	47.92

3 Experiments

3.1 Experimental Settings

Models. We conduct experiments using the widely adopted large language models Llama2, Llama3.x, and Mistral [39, 7, 15], focusing on models with over three billion parameters. The pruning targets include attention heads and FFN neurons, which are applied to the Transformer backbone. The `embed_tokens` and `lm_head` layers remain unchanged.

Calibration. For calibration, we consider FineWeb [31], a high-quality dataset curated from Common Crawl snapshots with rigorous deduplication and filtering. Specifically, we extract about 4M tokens (about 1k samples for a maximum input length of 4k) from its FineWeb-Edu subset to construct calibration samples, ensuring high data quality and efficiency.

Evaluation. We use perplexity as one evaluation metric for language comprehension performance [9], validated on the WikiText2 [27] test set. To evaluate the impact of compression across various downstream tasks, we report 0-shot accuracy on ARC [6], BoolQ [5], HellaSwag [49], OpenBookQA [28], RTE [41], and WinoGrande [33] tasks, as well as 5-shot accuracy on the MMLU [13] benchmark.

Implementation details. We implement Týr-the-Pruner with PyTorch [30] and leverage the HuggingFace Transformers and Datasets libraries [45] to manage models and datasets. For local pruning,

Table 2: **Post pruning performance on massive language models.** Accuracy (%), higher is better serves as the comparison metric. MMLU employed a 5-shot benchmark, while other tasks used 0-shot benchmarks. The percentage of average accuracy maintenance after pruning was recorded, with values $\geq 95\%$ highlighted in green and values $< 95\%$ in red. The best results are shown in **bold**.

Model	Sparsity	Method	Arc-C	Arc-E	BoolQ	HellaSwag	OBQA	RTE	WinoGrande	MMLU	AVG
Llama-2-70B	0%	N/A	54.44	82.74	83.73	64.77	37.40	67.87	77.98	68.79	67.22 (100%)
	50%	SliceGPT	38.65	68.39	69.63	38.40	25.00	63.54	67.40	50.20	52.65 (78%)
		LLM-Pruner	21.93	29.08	43.18	26.26	14.00	51.62	49.25	23.77	32.39 (48%)
		ZipLM	46.67	77.61	82.26	56.94	34.00	68.95	75.61	54.33	62.05 (92%)
		OSSCAR	48.21	78.37	81.99	57.00	32.60	67.15	76.64	56.05	62.25 (93%)
		FLAP	40.02	70.79	74.74	51.83	32.00	60.29	67.88	39.65	54.65 (81%)
		Týr-the-Pruner	48.21	79.12	83.18	60.04	35.20	70.76	78.14	60.58	64.40 (96%)
Llama-3.1-70B	0%	N/A	60.58	87.29	85.29	66.50	37.00	70.04	79.64	78.72	70.63 (100%)
	50%	SliceGPT	32.08	58.00	63.85	34.02	20.60	53.43	56.99	32.60	43.95 (62%)
		LLM-Pruner	21.42	25.38	38.81	26.22	13.80	54.87	50.83	24.95	32.04 (45%)
		ZipLM	48.55	78.54	80.55	55.98	31.60	66.79	78.37	62.73	62.89 (89%)
		OSSCAR	48.29	78.62	81.44	54.69	32.80	68.23	77.58	60.38	62.75 (89%)
		FLAP	37.54	68.90	67.34	43.98	26.40	60.65	72.30	54.40	53.94 (76%)
		Týr-the-Pruner	56.74	85.40	85.20	64.07	36.40	71.48	78.91	70.29	68.56 (97%)

we iteratively prune and adjust weights by removing one attention head or 16 FFN neurons at a time. The prune-and-search process consists of 4 iterations, where the sparsity interval at the i -th iteration is set to $12.5\% / 2^{i-1}$. In each iteration, we explore 50 generations with 128 offspring candidates per generation. The sparsity shifts of the attention or FFN layers are independent to ensure the consistency of the sparsity interval granularity. Candidate validation is performed using the distillation-inspired metric with vocabulary logits. We follow [36] to enhance validation efficiency: the 128 offspring are first validated on 2K tokens, and the top 16 are selected. These 16 survivors are then validated on 16K tokens, from which the top 4 are selected, and finally, the best one is validated and selected on 128K tokens. **To ensure a fair comparison**, we use the same FineWeb-Edu samples for calibration to reproduce the baselines. The benchmark results of the baselines may outperform their reported results due to the improved calibration sample size and data quality. All experiments for Týr-the-Pruner were conducted on 4 AMD Instinct™ MI250 (64GB) Accelerators, with models less than 13B parameters running on a single accelerator.

3.2 Performance

Language comprehension and downstream task performance of post-pruned LLMs. We applied structural pruning to various large language models using Týr-the-Pruner at overall sparsity levels of 12.5%, 25%, 37.5%, and 50%. The performance was benchmarked against state-of-the-art methods, including ShortGPT (layer pruning) [24], LaCO+ (ShortGPT with LaCO layer merging) [48], SliceGPT (embedding dimension pruning) [2], Wanda-SP [37, 1], LLM-Pruner [23], ZipLM [17], OSSCAR [26], and FLAP [1]. Table 1 summarizes the comparative results, highlighting post-pruning performance in language comprehension and downstream tasks (cf. Section A.8 for detailed results within each task).

Týr-the-Pruner demonstrates competitive performance across various sparsity ratios and LLMs. It consistently achieves state-of-the-art results at low sparsity ratios ($\leq 25\%$). For instance, pruning 12.5% of Llama-3-8B’s parameters yields the lowest perplexity (7.39) and the highest average downstream accuracy (62.37%), surpassing the previous advanced methods, LLM-Pruner and LaCO+, by 8.0% and 2.6%. At higher sparsities ($\geq 37.5\%$), maintaining performance poses a significant challenge for existing methods, with advanced techniques like OSSCAR often exhibiting perplexities exceeding 100 and accuracies dropping below 40%. Týr-the-Pruner, by contrast, excels under these conditions. For example, at 37.5% sparsity, the pruned Mistral-Nemo model achieves a perplexity of 11.47 and an accuracy of 55.63%, substantially outperforming ZipLM and FLAP.

Scale up to massive language models. Structural pruning of massive language models challenges post-pruned performance and resource budgets. We incorporated a CPU offload policy into typical baseline methods to ensure a fair comparison on 70B-scale models. Table 2 compares the post-pruning performance of Llama-2-70B and Llama-3.1-70B at 50% sparsity.

Experimental results demonstrate Týr-the-Pruner’s strong scalability under high sparsity for massive models. LLM-Pruner shows clear scaling limitations, maintaining only 48% accuracy when pruning

Table 3: **Inference efficiency of post-pruned LLMs with Týr-the-Pruner.** Benchmarks were conducted on a single AMD Instinct™ MI250 accelerator using PyTorch (HipBlas) for LLM inference, with input and output sequence lengths set to 2048.

Model	Sparsity	#Params	TTFT	Decode Throughput
Llama-3.1-8B	0%	8.0B	2.49 (1.00x)	12.27 (1.00x)
	25%	6.1B	1.94 (1.28x)	14.13 (1.15x)
	50%	4.3B	1.42 (1.75x)	16.97 (1.38x)
Mistral-Nemo	0%	14.3B	4.16 (1.00x)	6.68 (1.00x)
	25%	11.0B	3.34 (1.25x)	7.55 (1.13x)
	50%	7.8B	2.49 (1.67x)	8.93 (1.34x)

Llama-2-70B. In contrast, Týr-the-Pruner achieves 97% accuracy maintenance when pruning Llama-3.1-70B, outperforming alternative methods.

Inference efficiency of post-pruned LLMs. To evaluate the efficiency gains of post-pruned LLMs, we constructed inference benchmarks summarized in Table 3. For Llama-3.1-8B, 50% sparsity reduces time to first token (TTFT, in seconds) by 43% and boosts decode throughput (tokens/s) by 38%. These results highlight pruning as a key technique for inference optimization in large language models. More detailed efficiency analysis can be found in Section A.4.

3.3 Ablation Study

Prune-to-supernet. The effectiveness of local pruning and supernet construction depends on factors such as calibration samples, the implementation of local pruning, and error accumulation. Table 4 presents ablation study evaluating these factors for pruning Llama-3.1-8B at 50% sparsity. Experimental results show that FineWeb-Edu is consistently preferred as a calibration source, emphasizing the importance of selecting high-quality calibration samples. The presence of both first- and second-order optimization information and progressive pruning significantly impacts accuracy, demonstrating their necessity. Furthermore, the proposed expectation error accumulation approach outperforms alternatives, showcasing its ability to make sparse structures mutually aware appropriately.

Evolutionary search direction. To assess the impact of search direction on final performance, we compare the effects of minimizing single-task losses versus our similarity-based metric when pruning 50% of Llama-3.1-8B’s parameters, as shown in Table 5. Experiments show that single-task search underperforms our metric, which achieves optimal accuracy by calculating the similarity across activations from the first, median, last, and logits layers, requiring 96 GB for hidden activation checkpointing. Due to this overhead, the logits-only metric was favored, maintaining strong performance with reduced resource demands.

Effect comparison: Týr-the-Pruner vs. fine-grained search-only strategy. Figure 3 demonstrates the advantages of Týr-the-Pruner over the search-only strategy in efficacy and efficiency in identifying the optimal 50% sparsity distribution on Llama-3.1-8B. In which the search-only strategy uses a fine-grained 3.125% sparsity interval. Experimental results show that Týr-the-Pruner achieves a similar convergence trend as the search-only strategy but with faster convergence, fewer generations, and reduced search time. Additionally, the final post-pruned model discovered by Týr-the-Pruner outperforms the search-only strategy, with an average accuracy of 47.79 compared to 43.58. Our evolutionary search maintains time efficiency, with a single generation requiring only 190 seconds.

Table 4: **Ablation study on local pruning.** Wikitext2 perplexity and 0-shot accuracy on ARC-C, ARC-E, and BoolQ are reported.

Method	Configuration	Wikitext2 ARC-C ARC-E BoolQ			
		134.28	20.99	43.18	52.29
Local Pruning	Default	58.09	24.06	58.67	63.46
	Wikitext2 Calibrated	49.00	20.05	54.84	61.71
	C4 Calibrated	73.07	21.42	57.58	62.17
	w/o progressive pruning	63.48	23.38	56.65	62.17
Local Pruning & Build Supernet	w/o Hessian	109.88	22.53	51.68	46.48
	w/o Gradient	67.31	25.60	57.83	62.17
	Default	66.38	23.05	58.46	62.35
	w/o Error Accum.	538.23	21.93	33.54	40.31
Local Pruning & Build Supernet	w/ Random Error Accum.	208.92	22.70	39.14	45.05
	w/ Uniform Error Accum.	75.10	23.72	53.03	60.06

Table 5: **Ablation study on search direction.** Wikitext2 perplexity and 0-shot accuracy on ARC-C, ARC-E, BoolQ are reported.

Search Direction	Wikitext2	ARC-C	ARC-E	BoolQ
Wikitext2 Perplexity	17.22	29.69	64.06	62.23
Fineweb-Edu Perplexity	31.65	31.06	64.18	62.17
Similarity-based	28.56	32.51	65.87	63.12
Similarity-based Logits-only	30.89	31.83	65.36	64.62

Figure 3: Týr-the-Pruner has faster convergence, fewer exploration generations, shorter search time, and better search outcomes compared to the fine-grained search-only approach.

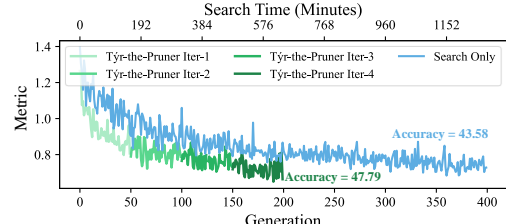


Figure 3: Týr-the-Pruner has faster convergence, fewer exploration generations, shorter search time, and better search outcomes compared to the fine-grained search-only approach.

Table 6: Týr-the-Pruner progressively refines and optimizes the sparsity distribution in iterations, steadily enhancing performance.

Method	Wikitext2	ARC-C	ARC-E	BoolQ	HellaSwag	OBQA	RTE	WinoGrande	MMLU	Avg
w/o search	66.38	23.55	58.46	62.35	32.51	16.60	51.26	52.88	28.34	40.74
search-only	27.96	25.34	59.30	64.71	36.52	22.20	55.23	56.20	29.17	43.58
Týr-the-Pruner I1	28.92	26.45	56.19	62.17	37.05	22.20	50.54	56.75	29.29	42.58
Týr-the-Pruner I2	31.80	29.27	62.54	63.51	38.18	23.80	50.54	56.85	30.23	44.37
Týr-the-Pruner I3	29.75	29.86	63.09	64.62	39.28	25.00	51.62	59.51	31.62	45.58
Týr-the-Pruner I4	30.89	31.83	65.36	66.64	39.99	24.80	58.12	61.80	33.76	47.79
Týr-the-Pruner I5	29.56	31.87	65.57	66.69	39.08	26.40	58.84	60.89	33.67	47.88

To further examine how Týr-the-Pruner refines model performance across successive iterations and to highlight its advantage over the search-only strategy, we report the 50% post-pruned results of Llama-3.1-8B on multiple tasks: Wikitext2 perplexity (\downarrow), 0-shot accuracy (\uparrow) on Arc, BoolQ, HellaSwag, OBQA, RTE, and WinoGrande, and 5-shot accuracy (\uparrow) on MMLU, as summarized in Table 6.

Experimental results underscore the superiority of Týr-the-Pruner compared to the search-only strategy. Under isotropic pruning, the w/o search baseline consistently delivers suboptimal performance across all tasks. By contrast, Týr-the-Pruner begins to surpass the search-only approach as early as the second iteration (I2), highlighting the advantage of progressively refining the sparsity distribution. The search-only method, constrained by the vast search space, suffers from extended search times and limited effectiveness. Týr-the-Pruner achieves an ideal result at the fourth iteration (I4). Although performance continues to improve at the fifth iteration (I5), the gains diminish, making four iterations the default configuration.

3.4 Compatibility with Quantization and Unstructured Sparsity

Týr-the-Pruner is compatible with further compression techniques. Table 7 reports results of applying quantization and unstructured sparsity to the 50% pruned Llama-3.1-8B model produced by Týr-the-Pruner. The results show that quantization preserves over 99% of the pruned model’s accuracy, while unstructured sparsity at 50% and 2:4 granularity achieves performance consistent with prior work [9, 25]. These findings indicate that Týr-the-Pruner provides a strong foundation for multi-stage compression pipelines, retaining both high accuracy and robustness to further compression.

Table 7: Quantization and unstructured sparsity applied to the 50% pruned Llama-3.1-8B with Týr-the-Pruner. Reported Wikitext2 perplexity and accuracy (%) across benchmarks.

Method	Wikitext2	Arc-C	Arc-E	BoolQ	HellaSwag	OBQA	RTE	WinoGrande	MMLU	Avg
Týr-the-Pruner @ FP16	30.89	31.83	65.36	66.64	39.99	24.80	58.12	61.80	33.76	47.79 (100%)
AWQ [21] @ W4A16	34.79	31.06	64.65	66.09	39.34	24.60	60.77	60.77	31.43	47.34 (%99.1)
SmoothQuant [47] @ W8A8	31.31	31.23	64.94	65.50	40.18	25.80	58.84	61.80	32.45	47.59 (%99.6)
RTN @ FP8E4M3	31.05	31.31	65.28	66.45	40.17	24.60	58.84	61.48	32.28	47.55 (%99.5)
SparseGPT [9] @ 50%	47.05	27.99	59.39	65.32	37.38	23.60	53.07	61.48	28.32	44.57 (%93.3)
ALPS [25] @ M4N2	70.22	23.04	53.62	63.43	34.22	21.40	52.71	58.17	27.34	41.74 (%87.3)

3.5 Memory/Storage Efficiency Analysis of Týr-the-Pruner

Týr-the-Pruner employs a supernet search technique, where storing a large-scale supernet in memory is costly. To address memory concerns, we optimize our approach by storing pruned substructures on disk instead of in high-bandwidth memory (HBM). An integer Python list is used to track the currently selected substructures, ensuring that only one entire LLM is loaded into HBM at any given time (e.g., the 7B model uses approximately 14GB, and the 13B model uses around 26GB). Table 8 provides detailed data on HBM and disk storage occupancy. Furthermore, since there is no dependency between iterations (iterative prune-and-search phase), the storage from previous iterations can be cleaned, further minimizing disk usage. Due to the low cost of disk storage, these memory and storage demands are highly acceptable.

Table 8: Resource requirements of Týr-the-Pruner.

Model Size	Submodules	HBM Usage	Disk Storage Usage
7-8B	576	14-16GB	39.6GB
13B	720	26GB	66.6GB
70B	1440	140GB	414.7GB

4 Related Work

Pruning techniques for compressing large language models. The growing complexity of Transformer-based language models, now reaching hundreds of billions of parameters, has intensified the necessity for effective pruning strategies. Pruning methods are generally divided into unstructural and structural approaches. Unstructural pruning [9, 37] achieves high accuracy by selectively zeroing individual elements in the weight. However, it often requires specialized hardware, such as 2:4 sparse tensor cores [52], for end-to-end acceleration. Structural pruning enables hardware-agnostic acceleration by removing entire weight groups, but it may result in a pronounced loss of accuracy.

Structural pruning of LLMs can be approached as local optimization, alleviating memory constraints from loading the full model. ZipLM [17] accelerates inference by leveraging the Optimal Brain Surgeon (OBS) [12] theory, pruning weights to minimize the impact on the Hessian matrix and adjusting the remaining weights to reduce layerwise loss. Building on ZipLM, OSSCAR [26] introduces a permutation search between pruned and remaining weights within each layer, further reducing pruning-induced loss. Some approaches apply global optimization strategies to prune LLMs, overcoming local constraints, enabling customized sparsity distributions, and potentially finding optimal solutions. Fisher information was introduced as a saliency metric to guide structure pruning via global dynamic programming [18]. LLM-Pruner [23] defines broad substructure dependency groups and then evaluates their saliency to guide pruning. FLAP [1] uses a global metric that considers both weights and activations for sparsity allocation, followed by layerwise pruning and bias adjustments to mitigate pruning losses.

Additionally, there is growing interest in embedding dimension [2] and depth [24, 48] pruning techniques for LLMs. Some training-aware structural pruning methods [50, 20, 29] are also gaining attention, as they further enhance pruning effectiveness by considering training dynamics.

Neural architecture search (NAS) for LLM compression. Several studies have applied NAS to compress LLMs, seeking architectures that reduce inference costs while maintaining accuracy. multi-objective NAS has been employed to explore various search space definitions, identifying compressed LLM architectures that enhance efficiency and accuracy when fine-tuned on specific downstream tasks [16]. LLaMAFlex [4] fine-tunes LLMs into supernets with a Gumbel softmax-based trainable subnet router, realized a “rain once, deploy many” model compression. EvoPress [36] proves that evolutionary search can determine suitable layerwise compression configurations and extends this method to support mixed-precision quantization and non-isotropic unstructural sparsity.

This paper presents a novel structural pruning framework, Týr-the-Pruner, for large language models. Unlike conventional methods, this framework searches for the optimal sparsity distribution within a supernet. Through enhanced supernet construction and an iterative prune-and-search technique, it achieves end-to-end global pruning optimization with strong efficiency and efficacy, setting a new benchmark for post-pruning accuracy maintenance.

5 Limitations

Týr-the-Pruner achieves state-of-the-art structural pruning outcomes by constructing reliable supernets and employing an iterative prune-and-search process. We have significantly reduced the search space and the number of generations explored. However, the search time cost remains non-negligible. Fair time costs in model compression are often considered acceptable, as the goal is to achieve a sufficiently optimized pruned model. However, we will continue to optimize it in future work.

6 Conclusion

This paper introduces Týr-the-Pruner, an end-to-end global structural pruning framework for large language models. By constructing a supernet through local pruning across various sparsity ratios and using evolutionary search to identify the optimal subnet, our framework achieves the optimal sparsity distribution under a target overall sparsity ratio. We propose an effective local pruning and an expectation error accumulation approach to enhance supernet construction. Additionally, an iterative prune-and-search strategy with coarse-to-fine sparsity granularity ensures rapid convergence. Extensive experiments show that Týr-the-Pruner outperforms state-of-the-art methods, achieving 50% parameter pruning while retaining 97% accuracy on Llama-3.1-70B.

References

- [1] Yongqi An, Xu Zhao, Tao Yu, Ming Tang, and Jinqiao Wang. Fluctuation-based adaptive structured pruning for large language models. In Michael J. Wooldridge, Jennifer G. Dy, and Sriraam Natarajan, editors, *Thirty-Eighth AAAI Conference on Artificial Intelligence, AAAI 2024, Thirty-Sixth Conference on Innovative Applications of Artificial Intelligence, IAAI 2024, Fourteenth Symposium on Educational Advances in Artificial Intelligence, EAAI 2014, February 20-27, 2024, Vancouver, Canada*, pages 10865–10873. AAAI Press, 2024.
- [2] Saleh Ashkboos, Maximilian L. Croci, Marcelo Gennari Do Nascimento, Torsten Hoefer, and James Hensman. Sliceprt: Compress large language models by deleting rows and columns. In *The Twelfth International Conference on Learning Representations, ICLR 2024, Vienna, Austria, May 7-11, 2024*. OpenReview.net, 2024.
- [3] Tom B. Brown, Benjamin Mann, Nick Ryder, Melanie Subbiah, Jared Kaplan, Prafulla Dhariwal, Arvind Neelakantan, Pranav Shyam, Girish Sastry, Amanda Askell, Sandhini Agarwal, Ariel Herbert-Voss, Gretchen Krueger, Tom Henighan, Rewon Child, Aditya Ramesh, Daniel M. Ziegler, Jeffrey Wu, Clemens Winter, Christopher Hesse, Mark Chen, Eric Sigler, Mateusz Litwin, Scott Gray, Benjamin Chess, Jack Clark, Christopher Berner, Sam McCandlish, Alec Radford, Ilya Sutskever, and Dario Amodei. Language models are few-shot learners. In Hugo Larochelle, Marc'Aurelio Ranzato, Raia Hadsell, Maria-Florina Balcan, and Hsuan-Tien Lin, editors, *Advances in Neural Information Processing Systems 33: Annual Conference on Neural Information Processing Systems 2020, NeurIPS 2020, December 6-12, 2020, virtual*, 2020.
- [4] Ruiqi Cai, Saurav Muralidharan, Hongxu Yin, Zhangyang Wang, Jan Kautz, and Pavlo Molchanov. Llamaflex: Many-in-one llms via generalized pruning and weight sharing. In *The Thirteenth International Conference on Learning Representations, ICLR 2025, Singapore, April 24-28, 2025*. OpenReview.net, 2025.
- [5] Christopher Clark, Kenton Lee, Ming-Wei Chang, Tom Kwiatkowski, Michael Collins, and Kristina Toutanova. Boolq: Exploring the surprising difficulty of natural yes/no questions. In Jill Burstein, Christy Doran, and Thamar Solorio, editors, *Proceedings of the 2019 Conference of the North American Chapter of the Association for Computational Linguistics: Human Language Technologies, NAACL-HLT 2019, Minneapolis, MN, USA, June 2-7, 2019, Volume 1 (Long and Short Papers)*, pages 2924–2936. Association for Computational Linguistics, 2019.
- [6] Peter Clark, Isaac Cowhey, Oren Etzioni, Tushar Khot, Ashish Sabharwal, Carissa Schoenick, and Oyvind Tafjord. Think you have solved question answering? try arc, the ai2 reasoning challenge. *arXiv:1803.05457v1*, 2018.
- [7] Abhimanyu Dubey, Abhinav Jauhri, Abhinav Pandey, Abhishek Kadian, Ahmad Al-Dahle, Aiesha Letman, Akhil Mathur, Alan Schelten, Amy Yang, Angela Fan, Anirudh Goyal, Anthony Hartshorn, Aobo Yang, Archi Mitra, Archie Sravankumar, Artem Korenev, Arthur Hinsvark, Arun Rao, Aston Zhang, Aurélien Rodriguez, Austen Gregerson, Ava Spataru, Baptiste Rozière, Bethany Biron, Binh Tang, Bobbie Chern, Charlotte Caucheteux, Chaya Nayak, Chloe Bi, Chris Marra, Chris McConnell, Christian Keller, Christophe Touret, Chunyang Wu, Corinne Wong, Cristian Canton Ferrer, Cyrus Nikolaidis, Damien Allonsius, Daniel Song, Danielle Pintz, Danny Livshits, David Esiobu, Dhruv Choudhary, Dhruv Mahajan, Diego Garcia-Olano, Diego Perino, Dieuwke Hupkes, Egor Lakomkin, Ehab AlBadawy, Elina Lobanova, Emily Dinan, Eric Michael Smith, Filip Radenovic, Frank Zhang, Gabriel Synnaeve, Gabrielle Lee, Georgia Lewis Anderson, Graeme Nail, Grégoire Mialon, Guan Pang, Guillem Cucurell, Hailey Nguyen, Hannah Korevaar, Hu Xu, Hugo Touvron, Iliyan Zarov, Imanol Arrieta Ibarra, Isabel M. Kloumann, Ishan Misra, Ivan Evtimov, Jade Copet, Jaewon Lee, Jan Geffert, Jana Vranes, Jason Park, Jay Mahadeokar, Jeet Shah, Jelmer van der Linde, Jennifer Billock, Jenny Hong, Jenya Lee, Jeremy Fu, Jianfeng Chi, Jianyu Huang, Jiawen Liu, Jie Wang, Jiecao Yu, Joanna Bitton, Joe Spisak, Jongsoo Park, Joseph Rocca, Joshua Johnstun, Joshua Saxe, Junteng Jia, Kalyan Vasudevan Alwala, Kartikeya Upasani, Kate Plawiak, Ke Li, Kenneth Heafield, Kevin Stone, and et al. The llama 3 herd of models. *CoRR*, abs/2407.21783, 2024.
- [8] Elias Frantar and Dan Alistarh. Optimal brain compression: A framework for accurate post-training quantization and pruning. In Sanmi Koyejo, S. Mohamed, A. Agarwal, Danielle Belgrave, K. Cho, and A. Oh, editors, *Advances in Neural Information Processing Systems 35: Annual Conference on Neural Information Processing Systems 2022, NeurIPS 2022, New Orleans, LA, USA, November 28 - December 9, 2022*, 2022.
- [9] Elias Frantar and Dan Alistarh. Sparseprt: Massive language models can be accurately pruned in one-shot. In Andreas Krause, Emma Brunskill, Kyunghyun Cho, Barbara Engelhardt, Sivan Sabato, and Jonathan Scarlett, editors, *International Conference on Machine Learning, ICML 2023, 23-29 July 2023, Honolulu, Hawaii, USA*, volume 202 of *Proceedings of Machine Learning Research*, pages 10323–10337. PMLR, 2023.

[10] Elias Frantar, Saleh Ashkboos, Torsten Hoefler, and Dan Alistarh. GPTQ: accurate post-training quantization for generative pre-trained transformers. *CoRR*, abs/2210.17323, 2022.

[11] Shangqian Gao, Chi-Heng Lin, Ting Hua, Zheng Tang, Yilin Shen, Hongxia Jin, and Yen-Chang Hsu. DISP-LLM: dimension-independent structural pruning for large language models. In Amir Globersons, Lester Mackey, Danielle Belgrave, Angela Fan, Ulrich Paquet, Jakub M. Tomczak, and Cheng Zhang, editors, *Advances in Neural Information Processing Systems 38: Annual Conference on Neural Information Processing Systems 2024, NeurIPS 2024, Vancouver, BC, Canada, December 10 - 15, 2024*, 2024.

[12] Babak Hassibi and David G. Stork. Second order derivatives for network pruning: Optimal brain surgeon. In Stephen Jose Hanson, Jack D. Cowan, and C. Lee Giles, editors, *Advances in Neural Information Processing Systems 5, [NIPS Conference, Denver, Colorado, USA, November 30 - December 3, 1992]*, pages 164–171. Morgan Kaufmann, 1992.

[13] Dan Hendrycks, Collin Burns, Steven Basart, Andy Zou, Mantas Mazeika, Dawn Song, and Jacob Steinhardt. Measuring massive multitask language understanding. *Proceedings of the International Conference on Learning Representations (ICLR)*, 2021.

[14] Edward J. Hu, Yelong Shen, Phillip Wallis, Zeyuan Allen-Zhu, Yuanzhi Li, Shean Wang, Lu Wang, and Weizhu Chen. Lora: Low-rank adaptation of large language models. In *The Tenth International Conference on Learning Representations, ICLR 2022, Virtual Event, April 25-29, 2022*. OpenReview.net, 2022.

[15] Albert Q. Jiang, Alexandre Sablayrolles, Arthur Mensch, Chris Bamford, Devendra Singh Chaplot, Diego de Las Casas, Florian Bressand, Gianna Lengyel, Guillaume Lample, Lucile Saulnier, Lélio Renard Lavaud, Marie-Anne Lachaux, Pierre Stock, Teven Le Scao, Thibaut Lavril, Thomas Wang, Timothée Lacroix, and William El Sayed. Mistral 7b. *CoRR*, abs/2310.06825, 2023.

[16] Aaron Klein, Jacek Golebiowski, Xingchen Ma, Valerio Perrone, and Cedric Archambeau. Structural pruning of large language models via neural architecture search. In *AutoML Conference 2023 (Workshop)*.

[17] Eldar Kurtic, Elias Frantar, and Dan Alistarh. Ziplm: Inference-aware structured pruning of language models. In Alice Oh, Tristan Naumann, Amir Globerson, Kate Saenko, Moritz Hardt, and Sergey Levine, editors, *Advances in Neural Information Processing Systems 36: Annual Conference on Neural Information Processing Systems 2023, NeurIPS 2023, New Orleans, LA, USA, December 10 - 16, 2023*, 2023.

[18] Woosuk Kwon, Sehoon Kim, Michael W. Mahoney, Joseph Hassoun, Kurt Keutzer, and Amir Gholami. A fast post-training pruning framework for transformers. In Sanmi Koyejo, S. Mohamed, A. Agarwal, Danielle Belgrave, K. Cho, and A. Oh, editors, *Advances in Neural Information Processing Systems 35: Annual Conference on Neural Information Processing Systems 2022, NeurIPS 2022, New Orleans, LA, USA, November 28 - December 9, 2022*, 2022.

[19] Qi Le, Enmao Diao, Ziyan Wang, Xinran Wang, Jie Ding, Li Yang, and Ali Anwar. Probe pruning: Accelerating llms through dynamic pruning via model-probing. *arXiv preprint arXiv:2502.15618*, 2025.

[20] Shengrui Li, Xuetong Han, and Jing Bai. Nuteprune: Efficient progressive pruning with numerous teachers for large language models. *CoRR*, abs/2402.09773, 2024.

[21] Ji Lin, Jiaming Tang, Haotian Tang, Shang Yang, Wei-Ming Chen, Wei-Chen Wang, Guangxuan Xiao, Xingyu Dang, Chuang Gan, and Song Han. AWQ: activation-aware weight quantization for on-device LLM compression and acceleration. In Phillip B. Gibbons, Gennady Pekhimenko, and Christopher De Sa, editors, *Proceedings of the Seventh Annual Conference on Machine Learning and Systems, MLSys 2024, Santa Clara, CA, USA, May 13-16, 2024*. mlsys.org, 2024.

[22] Yuqiao Liu, Yanan Sun, Bing Xue, Mengjie Zhang, Gary G Yen, and Kay Chen Tan. A survey on evolutionary neural architecture search. *IEEE transactions on neural networks and learning systems*, 34(2):550–570, 2021.

[23] Xinyin Ma, Gongfan Fang, and Xinchao Wang. Llm-pruner: On the structural pruning of large language models. In Alice Oh, Tristan Naumann, Amir Globerson, Kate Saenko, Moritz Hardt, and Sergey Levine, editors, *Advances in Neural Information Processing Systems 36: Annual Conference on Neural Information Processing Systems 2023, NeurIPS 2023, New Orleans, LA, USA, December 10 - 16, 2023*, 2023.

[24] Xin Men, Mingyu Xu, Qingyu Zhang, Bingning Wang, Hongyu Lin, Yaojie Lu, Xianpei Han, and Weipeng Chen. Shortgpt: Layers in large language models are more redundant than you expect. *CoRR*, abs/2403.03853, 2024.

[25] Xiang Meng, Kayhan Behdin, Haoyue Wang, and Rahul Mazumder. ALPS: improved optimization for highly sparse one-shot pruning for large language models. In Amir Globersons, Lester Mackey, Danielle Belgrave, Angela Fan, Ulrich Paquet, Jakub M. Tomczak, and Cheng Zhang, editors, *Advances in Neural Information Processing Systems 38: Annual Conference on Neural Information Processing Systems 2024, NeurIPS 2024, Vancouver, BC, Canada, December 10 - 15, 2024*, 2024.

[26] Xiang Meng, Shibal Ibrahim, Kayhan Behdin, Hussein Hazimeh, Natalia Ponomareva, and Rahul Mazumder. OSSCAR: one-shot structured pruning in vision and language models with combinatorial optimization. In *Forty-first International Conference on Machine Learning, ICML 2024, Vienna, Austria, July 21-27, 2024*. OpenReview.net, 2024.

[27] Stephen Merity, Caiming Xiong, James Bradbury, and Richard Socher. Pointer sentinel mixture models. In *5th International Conference on Learning Representations, ICLR 2017, Toulon, France, April 24-26, 2017, Conference Track Proceedings*. OpenReview.net, 2017.

[28] Todor Mihaylov, Peter Clark, Tushar Khot, and Ashish Sabharwal. Can a suit of armor conduct electricity? a new dataset for open book question answering. In *EMNLP*, 2018.

[29] Saurav Muralidharan, Sharath Turuvekere Sreenivas, Raviraj Joshi, Marcin Chochowski, Mostafa Patwary, Mohammad Shoeybi, Bryan Catanzaro, Jan Kautz, and Pavlo Molchanov. Compact language models via pruning and knowledge distillation. *CoRR*, abs/2407.14679, 2024.

[30] Adam Paszke, Sam Gross, Francisco Massa, Adam Lerer, James Bradbury, Gregory Chanan, Trevor Killeen, Zeming Lin, Natalia Gimelshein, Luca Antiga, Alban Desmaison, Andreas Köpf, Edward Z. Yang, Zachary DeVito, Martin Raison, Alykhan Tejani, Sasank Chilamkurthy, Benoit Steiner, Lu Fang, Junjie Bai, and Soumith Chintala. Pytorch: An imperative style, high-performance deep learning library. In Hanna M. Wallach, Hugo Larochelle, Alina Beygelzimer, Florence d'Alché-Buc, Emily B. Fox, and Roman Garnett, editors, *Advances in Neural Information Processing Systems 32: Annual Conference on Neural Information Processing Systems 2019, NeurIPS 2019, December 8-14, 2019, Vancouver, BC, Canada*, pages 8024–8035, 2019.

[31] Guilherme Penedo, Hynek Kydlícek, Loubna Ben Allal, Anton Lozhkov, Margaret Mitchell, Colin Raffel, Leandro von Werra, and Thomas Wolf. The fineweb datasets: Decanting the web for the finest text data at scale. *CoRR*, abs/2406.17557, 2024.

[32] Baolin Peng, Chunyuan Li, Pengcheng He, Michel Galley, and Jianfeng Gao. Instruction tuning with gpt-4. *arXiv preprint arXiv:2304.03277*, 2023.

[33] Keisuke Sakaguchi, Ronan Le Bras, Chandra Bhagavatula, and Yejin Choi. Winogrande: An adversarial winograd schema challenge at scale. *arXiv preprint arXiv:1907.10641*, 2019.

[34] Noam Shazeer. GLU variants improve transformer. *CoRR*, abs/2002.05202, 2020.

[35] Xuan Shen, Pu Zhao, Yifan Gong, Zhenglun Kong, Zheng Zhan, Yushu Wu, Ming Lin, Chao Wu, Xue Lin, and Yanzhi Wang. Search for efficient large language models. In Amir Globersons, Lester Mackey, Danielle Belgrave, Angela Fan, Ulrich Paquet, Jakub M. Tomczak, and Cheng Zhang, editors, *Advances in Neural Information Processing Systems 38: Annual Conference on Neural Information Processing Systems 2024, NeurIPS 2024, Vancouver, BC, Canada, December 10 - 15, 2024*, 2024.

[36] Oliver Sieberling, Denis Kuznedelev, Eldar Kurtic, and Dan Alistarh. EvoPress: Accurate dynamic model compression via evolutionary search. In Aarti Singh, Maryam Fazel, Daniel Hsu, Simon Lacoste-Julien, Felix Berkenkamp, Tegan Maharaj, Kiri Wagstaff, and Jerry Zhu, editors, *Proceedings of the 42nd International Conference on Machine Learning*, volume 267 of *Proceedings of Machine Learning Research*, pages 55556–55590. PMLR, 13–19 Jul 2025.

[37] Mingjie Sun, Zhuang Liu, Anna Bair, and J. Zico Kolter. A simple and effective pruning approach for large language models. In *The Twelfth International Conference on Learning Representations, ICLR 2024, Vienna, Austria, May 7-11, 2024*. OpenReview.net, 2024.

[38] Shengkun Tang, Oliver Sieberling, Eldar Kurtic, Zhiqiang Shen, and Dan Alistarh. Darwinlm: Evolutionary structured pruning of large language models. *arXiv preprint arXiv:2502.07780*, 2025.

[39] Hugo Touvron, Louis Martin, Kevin Stone, Peter Albert, Amjad Almahairi, Yasmine Babaei, Nikolay Bashlykov, Soumya Batra, Prajjwal Bhargava, Shruti Bhosale, Dan Bikel, Lukas Blecher, Cristian Canton-Ferrer, Moya Chen, Guillem Cucurull, David Esiobu, Jude Fernandes, Jeremy Fu, Wenjin Fu, Brian Fuller, Cynthia Gao, Vedanuj Goswami, Naman Goyal, Anthony Hartshorn, Saghar Hosseini, Rui Hou, Hakan Inan, Marcin Kardas, Viktor Kerkez, Madiam Khabsa, Isabel Kloumann, Artem Korenev, Punit Singh Koura, Marie-Anne Lachaux, Thibaut Lavril, Jenya Lee, Diana Liskovich, Yinghai Lu, Yuning Mao,

Xavier Martinet, Todor Mihaylov, Pushkar Mishra, Igor Molybog, Yixin Nie, Andrew Poulton, Jeremy Reizenstein, Rashi Rungta, Kalyan Saladi, Alan Schelten, Ruan Silva, Eric Michael Smith, Ranjan Subramanian, Xiaoqing Ellen Tan, Binh Tang, Ross Taylor, Adina Williams, Jian Xiang Kuan, Puxin Xu, Zheng Yan, Iliyan Zarov, Yuchen Zhang, Angela Fan, Melanie Kambadur, Sharan Narang, Aurélien Rodriguez, Robert Stojnic, Sergey Edunov, and Thomas Scialom. Llama 2: Open foundation and fine-tuned chat models. [CoRR](#), abs/2307.09288, 2023.

[40] Ashish Vaswani, Noam Shazeer, Niki Parmar, Jakob Uszkoreit, Llion Jones, Aidan N. Gomez, Łukasz Kaiser, and Illia Polosukhin. Attention is all you need. In Isabelle Guyon, Ulrike von Luxburg, Samy Bengio, Hanna M. Wallach, Rob Fergus, S. V. N. Vishwanathan, and Roman Garnett, editors, *Advances in Neural Information Processing Systems 30: Annual Conference on Neural Information Processing Systems 2017, December 4-9, 2017, Long Beach, CA, USA*, pages 5998–6008, 2017.

[41] Alex Wang, Amanpreet Singh, Julian Michael, Felix Hill, Omer Levy, and Samuel R. Bowman. GLUE: A multi-task benchmark and analysis platform for natural language understanding. In *7th International Conference on Learning Representations, ICLR 2019, New Orleans, LA, USA, May 6-9, 2019*. OpenReview.net, 2019.

[42] Boyao Wang, Rui Pan, Shizhe Diao, Xingyuan Pan, Jipeng Zhang, Renjie Pi, and Tong Zhang. Adapt-pruner: Adaptive structural pruning for efficient small language model training. [CoRR](#), abs/2502.03460, 2025.

[43] Xin Wang, Yu Zheng, Zhongwei Wan, and Mi Zhang. SVD-LLM: truncation-aware singular value decomposition for large language model compression. [CoRR](#), abs/2403.07378, 2024.

[44] Yuxin Wang, Minghua Ma, Zekun Wang, Jingchang Chen, Liping Shan, Qing Yang, Dongliang Xu, Ming Liu, and Bing Qin. CFSP: an efficient structured pruning framework for llms with coarse-to-fine activation information. In Owen Rambow, Leo Wanner, Marianna Apidianaki, Hend Al-Khalifa, Barbara Di Eugenio, and Steven Schockaert, editors, *Proceedings of the 31st International Conference on Computational Linguistics, COLING 2025, Abu Dhabi, UAE, January 19-24, 2025*, pages 9311–9328. Association for Computational Linguistics, 2025.

[45] Thomas Wolf, Lysandre Debut, Victor Sanh, Julien Chaumond, Clement Delangue, Anthony Moi, Pierrick Cistac, Tim Rault, Rémi Louf, Morgan Funtowicz, Joe Davison, Sam Shleifer, Patrick von Platen, Clara Ma, Yacine Jernite, Julien Plu, Canwen Xu, Teven Le Scao, Sylvain Gugger, Mariama Drame, Quentin Lhoest, and Alexander M. Rush. Transformers: State-of-the-art natural language processing. In Qun Liu and David Schlangen, editors, *Proceedings of the 2020 Conference on Empirical Methods in Natural Language Processing: System Demonstrations, EMNLP 2020 - Demos, Online, November 16-20, 2020*, pages 38–45. Association for Computational Linguistics, 2020.

[46] Shangyu Wu, Hongchao Du, Ying Xiong, Shuai Chen, Tei-Wei Kuo, Nan Guan, and Chun Jason Xue. Evop: Robust LLM inference via evolutionary pruning. [CoRR](#), abs/2502.14910, 2025.

[47] Guangxuan Xiao, Ji Lin, Mickaël Seznec, Hao Wu, Julien Demouth, and Song Han. Smoothquant: Accurate and efficient post-training quantization for large language models. In Andreas Krause, Emma Brunskill, Kyunghyun Cho, Barbara Engelhardt, Sivan Sabato, and Jonathan Scarlett, editors, *International Conference on Machine Learning, ICML 2023, 23-29 July 2023, Honolulu, Hawaii, USA*, volume 202 of *Proceedings of Machine Learning Research*, pages 38087–38099. PMLR, 2023.

[48] Yifei Yang, Zouying Cao, and Hai Zhao. Laco: Large language model pruning via layer collapse. In Yaser Al-Onaizan, Mohit Bansal, and Yun-Nung Chen, editors, *Findings of the Association for Computational Linguistics: EMNLP 2024, Miami, Florida, USA, November 12-16, 2024*, pages 6401–6417. Association for Computational Linguistics, 2024.

[49] Rowan Zellers, Ari Holtzman, Yonatan Bisk, Ali Farhadi, and Yejin Choi. Hellaswag: Can a machine really finish your sentence? In *Proceedings of the 57th Annual Meeting of the Association for Computational Linguistics*, 2019.

[50] Mingyang Zhang, Hao Chen, Chunhua Shen, Zhen Yang, Linlin Ou, Xinyi Yu, and Bohan Zhuang. Loraprune: Structured pruning meets low-rank parameter-efficient fine-tuning. In Lun-Wei Ku, Andre Martins, and Vivek Srikumar, editors, *Findings of the Association for Computational Linguistics, ACL 2024, Bangkok, Thailand and virtual meeting, August 11-16, 2024*, pages 3013–3026. Association for Computational Linguistics, 2024.

[51] Wayne Xin Zhao, Kun Zhou, Junyi Li, Tianyi Tang, Xiaolei Wang, Yupeng Hou, Yingqian Min, Beichen Zhang, Junjie Zhang, Zican Dong, Yifan Du, Chen Yang, Yushuo Chen, Zhipeng Chen, Jinhao Jiang, Ruiyang Ren, Yifan Li, Xinyu Tang, Zikang Liu, Peiyu Liu, Jian-Yun Nie, and Ji-Rong Wen. A survey of large language models. [CoRR](#), abs/2303.18223, 2023.

[52] Aojun Zhou, Yukun Ma, Junnan Zhu, Jianbo Liu, Zhijie Zhang, Kun Yuan, Wenxiu Sun, and Hongsheng Li. Learning N: M fine-grained structured sparse neural networks from scratch. In 9th International Conference on Learning Representations, ICLR 2021, Virtual Event, Austria, May 3-7, 2021. OpenReview.net, 2021.

A Appendix

A.1 Theoretical Foundations of Local Pruning

Redundant channel identification. We consider first- and second-order terms to minimize Equation (3). For the first-order term, we identify the to-prune channel p by $\operatorname{argmin}_{\mathbf{W}_{p,:}} (|\mathbf{G}_{p,:} \mathbf{W}_{p,:}^\top|)$, which identifies the weights with the minimal contribution in the gradient direction [23]. For the second-order term, we employ the Optimal Brain Surgeon (OBS) method [12], which optimizes $\operatorname{argmin}_{\mathbf{W}_{p,:}} \left(\frac{\|\mathbf{W}_{p,:}\|_2^2}{2[\mathbf{H}^{-1}]_{p,p}} \right)$ by considering the inverse of the diagonal elements of the Hessian matrix. This method measures each channel's contribution to the curvature of the loss function.

The identification metric for redundant channels is derived from a manual design that takes into account both first- and second-order optimization information, distinguishing it from previous work. Table 4 demonstrates the validity of our metric by ablation.

Weight adjustment. We minimize Equation (3) by applying the Lagrange multiplier method to impose constraints on the p -th channel should be pruned ($\delta \mathbf{W}_{p,:} = \mathbf{W}_{p,:}$):

$$\mathcal{L}(\delta \mathbf{W}, \boldsymbol{\lambda}) = \mathbf{G}^\top \delta \mathbf{W} + \frac{1}{2} \delta \mathbf{W}^\top \mathbf{H} \delta \mathbf{W} + \boldsymbol{\lambda}^\top (\delta \mathbf{W}_{p,:} - \mathbf{W}_{p,:}). \quad (7)$$

Under the constraints, the resulting loss function $\mathcal{L}(\delta \mathbf{W}, \boldsymbol{\lambda})$ will be differentiated with respect to $\delta \mathbf{W}$ and $\boldsymbol{\lambda}$ to find the minimum value:

$$\begin{cases} \frac{\partial \mathcal{L}(\delta \mathbf{W}, \boldsymbol{\lambda})}{\partial \delta \mathbf{W}} = \mathbf{G} + \mathbf{H} \delta \mathbf{W} + \mathbf{E}_p \boldsymbol{\lambda}^\top = \mathbf{0}, \\ \frac{\partial \mathcal{L}(\delta \mathbf{W}, \boldsymbol{\lambda})}{\partial \boldsymbol{\lambda}} = \delta \mathbf{W}_{p,:} - \mathbf{W}_{p,:} = \mathbf{0}. \end{cases} \quad (8)$$

For the $\mathbf{G} + \mathbf{H} \delta \mathbf{W} + \mathbf{E}_p \boldsymbol{\lambda}^\top$ term, we use p and $\sim p$ to denote channels to prune and channels to remain. Corresponding variables can be expanded in this way:

$$\begin{bmatrix} \mathbf{G}_{p,:} \\ \mathbf{G}_{\sim p,:} \end{bmatrix} + \begin{bmatrix} \mathbf{H}_{p,p} & \mathbf{H}_{p,\sim p} = \mathbf{0} \\ \mathbf{H}_{\sim p,p} = \mathbf{0} & \mathbf{H}_{\sim p,\sim p} \end{bmatrix} \begin{bmatrix} \delta \mathbf{W}_{p,:} \\ \delta \mathbf{W}_{\sim p,:} \end{bmatrix} + \begin{bmatrix} \boldsymbol{\lambda}^\top \\ \mathbf{0} \end{bmatrix} = \mathbf{0}, \quad (9)$$

where the elements of the Hessian matrix corresponding to the pruned positions p can be set to zero (when a channel of the weights is pruned, the same position of the Hessian/invHessian matrix are pruned correspondingly [8]). Overall, the solution is $\delta \mathbf{W}_{\sim p,:} = -\mathbf{H}_{\sim p,\sim p}^{-1} \mathbf{G}_{\sim p,:}$.

Fast update of inverse Hessian matrix. When the p -th channel is pruned, the inverse Hessian matrix \mathbf{H}^{-1} must be updated to account for the removal of the corresponding channel p in \mathbf{W} . This update can be efficiently derived by leveraging the properties of partitioned matrices and applying the Sherman-Morrison-Woodbury formula. The main idea is that the pruning of the p -th channel results in a rank-1 update to \mathbf{H}^{-1} , which is mathematically represented as:

$$\mathbf{H}^{-1} \leftarrow \mathbf{H}^{-1} - \frac{1}{[\mathbf{H}^{-1}]_{pp}} \mathbf{H}_{:,p}^{-1} \mathbf{H}_{p,:}^{-1}. \quad (10)$$

By updating the inverse Hessian with a rank-1 adjustment, the influence of the p -th channel is properly removed through the outer product of the corresponding column and row vectors, using the reciprocal of the p -th diagonal element. The updated \mathbf{H}^{-1} ensures consistency for the remaining channels, enabling efficient and scalable pruning operations. This method has a time complexity of $O(d_{in}^2)$, avoiding full recomputation of the inverse and ensuring computational efficiency.

A.2 Algorithms for Týr-the-Pruner

Algorithm 1 Function local_pruning

```

1: Inputs: to-prune weight  $\mathbf{W}$ ,
   input activations  $\mathbf{X}$ ,
   sparsity  $S$ ,
   pruning granularity (pruning times)  $K$ 
2: Mask  $\leftarrow$  ones_like( $\mathbf{W}$ )
3:  $\mathbf{H} \leftarrow \mathbf{X}^\top \mathbf{X}$ 
4:  $\mathbf{G} \leftarrow \mathbf{H}\mathbf{W}$ 
5: for  $k \leftarrow 1$  to  $K$  do
6:    $p \leftarrow \operatorname{argmin}_p \left( |\mathbf{G}_{p,:} \mathbf{W}_{p,:}^\top| + \frac{\|\mathbf{W}_{p,:}\|_2^2}{2[\mathbf{H}^{-1}]_{p,p}} \right)$ 
7:   Mask $p$   $\leftarrow 0$ 
8:    $\mathbf{W}_{\sim p,:} \leftarrow \mathbf{W}_{\sim p,:} + \mathbf{H}_{\sim p,\sim p}^{-1} \mathbf{G}_{\sim p,:}$ 
9:    $\mathbf{H}^{-1} \leftarrow \mathbf{H}^{-1} - \frac{1}{[\mathbf{H}^{-1}]_{p,p}} \mathbf{H}_{:,p}^{-1} \mathbf{H}_{p,:}^{-1}$ 
10: end for
11: Return  $\mathbf{Mask} \odot \mathbf{W}$ 

```

Algorithm 2 Function prune_to_supernet

```

1: Inputs: LLM weights  $\{\mathbf{W}_1, \mathbf{W}_2, \dots, \mathbf{W}_L\}$ ,
   sparsity ratios
    $\{S_{1,1}, \dots, S_{1,E}, \dots, S_{L,E}\}$ ,
   input activations for first weight  $\mathbf{X}$ ,
   pruning granularity (pruning times)  $K$ 
2: for  $\ell \leftarrow 1$  to  $L$  do
3:    $\mathbf{X}_{\text{list}} \leftarrow []$ 
4:   for  $e \leftarrow 1$  to  $E$  do
5:      $\widehat{\mathbf{W}}_{\ell,e} \leftarrow \text{local\_pruning}(\mathbf{W}_\ell, \mathbf{X}, S_{\ell,e}, K)$ 
6:     store( $\widehat{\mathbf{W}}_{\ell,e}$ )
7:      $\mathbf{X}_{\text{list}}. \text{append}(\mathbf{X} \cdot \widehat{\mathbf{W}}_{\ell,e})$ 
8:   end for
9:    $\mathbf{X} \leftarrow \sum_{e=1}^E \frac{1-S_{\ell,e}}{\sum_{e=1}^E (1-S_{\ell,e})} \mathbf{X}_{\text{list}}[e]$ 
10: end for
11: Return  $\{\widehat{\mathbf{W}}_{\ell,e}\}_{\ell=1,e=1}^{L,E}$ 

```

Algorithm 3 Function evolutionary_search

```

1: Inputs: sparse structures  $\mathbb{W} = \{\mathbf{W}_{1,1}, \dots, \mathbf{W}_{1,E}, \dots, \mathbf{W}_{L,E}\}$ ,
   sparsity ratios  $\{S_\ell\}_{\ell=1}^L$ , sparsity interval  $S^g$ 
2: procedure makeCandidates( $\text{numCandidates}$ ,  $\mathbb{W}$ ,  $\{S_\ell\}_{\ell=1}^L$ ,  $S^g$ )
3:    $\text{Candidates} \leftarrow []$ 
4:   for  $i \leftarrow 1$  to  $\text{numCandidates}$  do
5:      $\text{Candidates}. \text{append}(\text{randSparsityShift}(\mathbb{W}, \{S_\ell\}_{\ell=1}^L, S^g, \text{randChoice}(L), \text{randChoice}(L)))$ 
6:   end for
7: end procedure: return  $\text{Candidates}$ 
8:  $\{\widehat{S}_\ell\}_{\ell=1}^L \leftarrow \{S_\ell\}_{\ell=1}^L$ 
9: for  $g \leftarrow 1$  to  $\text{numGenerations}$  do
10:    $\text{Offsprings} \leftarrow \text{makeCandidates}(\text{numCandidates}, \mathbb{W}, \{\widehat{S}_\ell\}_{\ell=1}^L, S^g)$ 
11:    $\{\widehat{S}_\ell\}_{\ell=1}^L \leftarrow \text{checkSparsity}(\operatorname{argminSearchMetric}(\text{Offsprings}))$ 
12: Return  $\{\widehat{S}_\ell\}_{\ell=1}^L$ 

```

Algorithm 4 Function Týr-the-Pruner

```

1: Inputs: LLM weights  $\{\mathbf{W}_1, \mathbf{W}_2, \dots, \mathbf{W}_L\}$ , input activations for first weight  $\mathbf{X}$ ,
   pruning granularity (pruning times)  $K$ , overall sparsity  $S$ , sparsity interval  $S^g$ ,
   num sparse structures  $E$ , iterations  $T$ 
2: procedure generateSparsities( $L, E, \{S_\ell\}_{\ell=1}^L, S^g$ )
3:    $\text{Sparsities} = []$ 
4:   for  $\ell \leftarrow 0$  to  $\text{range}(L)$  do
5:     for  $e \leftarrow 0$  to  $\text{range}(E)$  do
6:        $\text{Sparsities}. \text{append}(S_\ell - ((e - 1) \times 0.5) \times S^g + i \times S^g)$ 
7:     end for
8:   end for
9: end procedure: return  $\text{Sparsities}$ 
10:  $\{\widehat{S}_\ell\}_{\ell=1}^L \leftarrow \{S\}_L$ 
11: for  $t \leftarrow 1$  to  $T$  do
12:    $\text{Sparsities} \leftarrow \text{generateSparsities}(L, E, \{\widehat{S}_\ell\}_{\ell=1}^L, S^g)$ 
13:    $\{\widehat{\mathbf{W}}_{\ell,e}\}_{\ell=1,e=1}^{L,E} \leftarrow \text{prune\_to\_supernet}(\{\mathbf{W}_\ell\}_{\ell=1}^L, \text{Sparsities}, \mathbf{X}, K)$ 
14:    $\{\widehat{S}_\ell\}_{\ell=1}^L \leftarrow \text{evolutionary\_search}(\{\widehat{\mathbf{W}}_{\ell,e}\}_{\ell=1,e=1}^{L,E}, \{\widehat{S}_\ell\}_{\ell=1}^L, S^g)$ 
15:    $S^g \leftarrow S^g \times 0.5$ 
16: end for
17: Return compress( $\{\widehat{\mathbf{W}}_{\ell,e}\}_{\ell=1,e=1}^{L,E}$ ,  $\{\widehat{S}_\ell\}_{\ell=1}^L$ )

```

A.3 Further Comparisons

To further demonstrate the effectiveness of our proposed method, Týr-the-Pruner, we conducted a more comprehensive comparison. The competitors include the pure subnet search framework SearchLLM [35], the probe-based dynamic pruning approach ProbePruning [19], the sparsity distribution optimizer Adapt-Pruner [42], the coarse-and-fine combined approach CFSP [44], the calibration-free approach PruneNet [19], the structure-independent approach DISP-LLM [11], the cluster-based evolutionary pruning approach EvoP [46], and the search-only approach DarwinLLM [38]. The experimental results, with competitor performance taken from their respective papers, are presented in Table 9.

It is evident that Týr-the-Pruner significantly outperforms other structured pruning methods, achieving better performance even at higher sparsities compared to other methods at lower sparsities. In particular, Týr-the-Pruner surpasses the search-based methods SearchLLM, EvoP, and DarwinLLM, demonstrating the effectiveness of our effective local pruning approach, expected error accumulation, and iterative prune-and-search strategy.

A.4 Efficiency Analysis on Non-isotropic Structural Pruning

Large language models (LLMs) with non-isotropic pruning may be considered to exhibit inferior inference efficiency compared to those with isotropic sparsity across layers. To explore, we provide a comparative analysis of inference efficiency for Llama-3.1-8B and Mistral-Nemo, both pre- and post-50% structural pruning. The evaluation was conducted on an AMD Instinct™ MI250 Accelerator using Pytorch (HipBlas), covering both prefilling and decoding tasks across a range of sentence lengths, as illustrated in Figure 4.

The variance (Var) quantifies the degree of variation in sparsity under non-isotropic pruning conditions; a larger variance indicates more fluctuation in sparsity across layers. As shown in Figure 4, the 50% structural pruned LLMs achieve up to 1.3x or greater speedup in both prefilling and decoding tasks compared to their dense counterparts across most sentence lengths. Variations in layer sparsity do not have a significant impact on efficiency. A slight efficiency decrease is only observed when the variance reaches 1. In this case, the reduction in efficiency is likely due to the frequent high sparsity, which leads to more memory-bottlenecked “thin” matrix multiplications in the computational graph.

Figure 5(a) and Figure 5(b) compare the sparsity distributions of the MHA and FFN layers in Llama-3.1-8B after 50% pruning with Týr-the-Pruner and the search-only methods, respectively. The sparsity distribution obtained by Týr-the-Pruner resembles that of the search-only strategy, yet Týr-the-Pruner performs better. Its search process is more refined, incorporating multiple rounds of expectation error accumulation, ultimately leading to a superior sparsity distribution and higher performance in the pruned model.

Figure 5(c) and Figure 5(d) compare the sparsity distributions of the MHA and FFN layers in the 50% post-pruned Llama-3.1-8B across different iterations of Týr-the-Pruner. Týr-the-Pruner identifies a

Table 9: **Further comparisons.** Perplexity on Wikitext2 (lower is better) and 0-shot accuracy (%), higher is better, DarwinLLM reported the 25-shot Arc-C benchmark) serve as the comparison metrics. Optimal results are **bolded**.

Model	Sparsity	Method	Wikitext2 ↓	BoolQ ↑	WinoGrande ↑	ARC-E ↑	ARC-C ↑
Llama-7B	0%	N/A	5.68	71.38	67.01	67.45	41.38
	20%	SearchLLM	6.89	70.98	74.92	64.23	36.52
	25%	Týr-the-Pruner	7.36	75.81	75.68	66.36	42.06
Llama-2-7B	0%	N/A	5.12	77.68	69.06	76.30	43.43
	30%	PruneNet	-	-	61.09	53.20	33.53
		DISP-LLM	6.85	-	62.27	59.81	33.19
Llama-2-13B	37.5%	Týr-the-Pruner	10.29	68.87	66.93	71.13	38.31
	40%	ProbePruning	8.01	64.70	58.10	62.50	37.70
		DISP-LLM	9.84	-	58.41	43.06	25.85
Llama-3.1-8B	30%	DISP-LLM	5.77	-	62.70	55.80	63.30
		DarwinLLM	-	-	55.80	38.10	
		Týr-the-Pruner	16.17	65.54	62.12	66.12	33.62
Llama-3-8B	0%	N/A	4.57	80.61	72.22	79.46	48.46
	20%	EvoP	6.33	-	68.00	73.00	40.00
	25%	Týr-the-Pruner	5.79	81.35	72.06	77.74	44.97
Llama-3.1-8B	30%	DISP-LLM	5.77	-	66.85	63.80	39.42
	37.5%	Týr-the-Pruner	7.17	80.76	72.06	76.35	43.26
		CFSP	-	-	64.17	62.33	38.05
Llama-3-8B	50%	DISP-LLM	7.11	-	59.27	52.57	33.28
		Týr-the-Pruner	9.59	74.46	70.09	72.18	39.85
	0%	N/A	5.84	82.17	73.56	81.31	51.54
Llama-3.1-8B	40%	Adapt-Pruner	33.75	-	56.75	45.16	25.97
	50%	DarwinLLM	-	62.20	57.30	59.60	34.20
		Týr-the-Pruner	30.89	66.64	61.80	65.86	31.83
Llama-3-8B	0%	N/A	5.76	81.10	73.01	80.05	50.43
	40%	MLP-only	14.90	70.30	67.20	57.40	39.00
	25%	ProbePruning	13.14	76.02	71.11	75.63	42.15

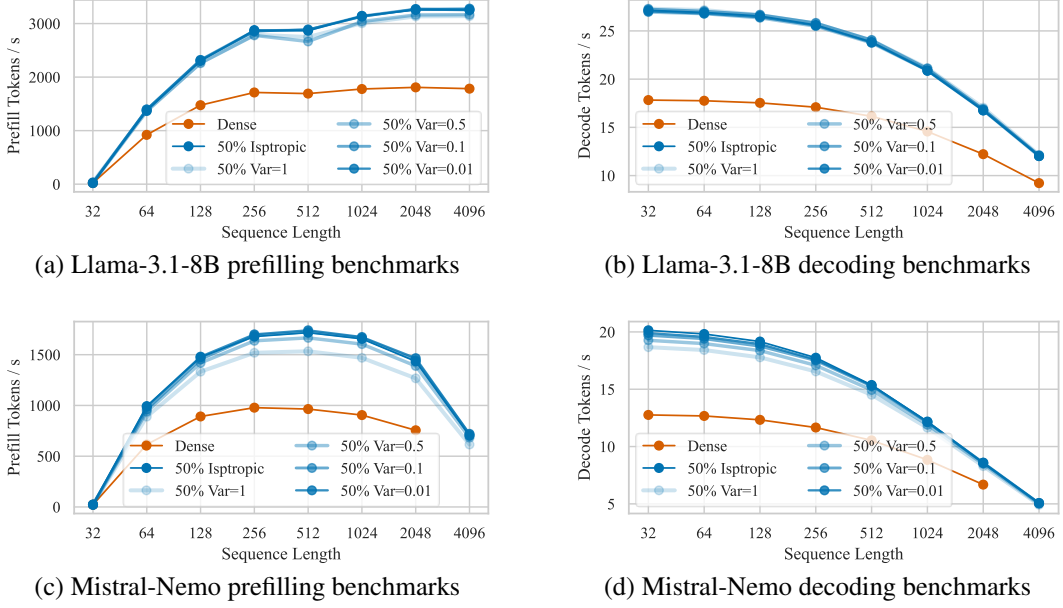


Figure 4: Pre- and post-pruning large language model inference benchmarks.

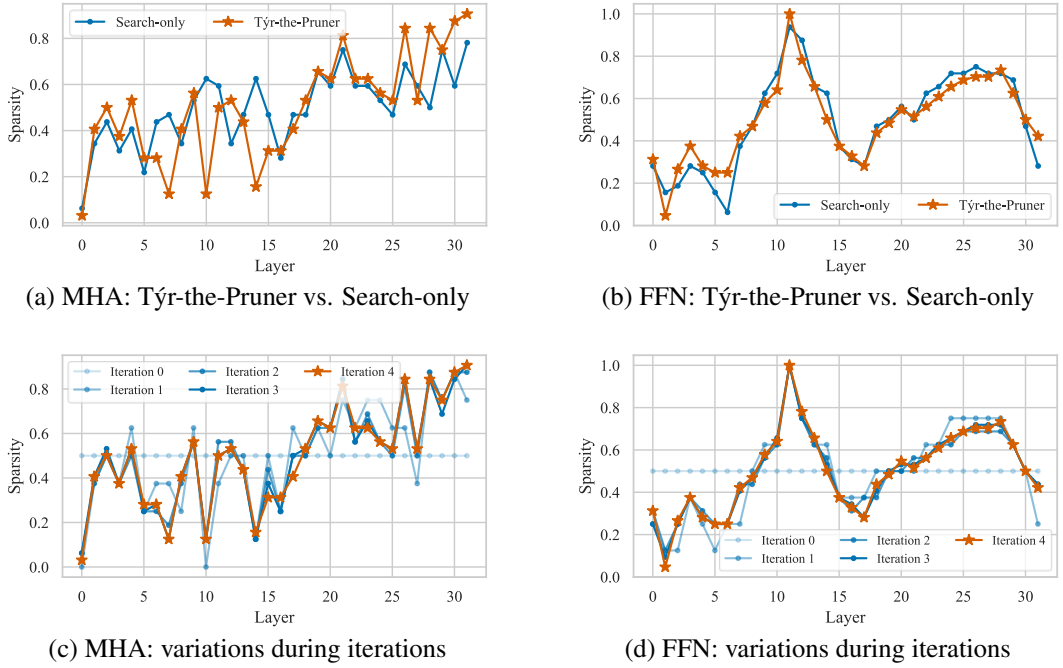


Figure 5: Sparsity distribution of Týr-the-Pruner and the search-only strategy on Llama-3.1-8B.

relatively ideal and coarse-grained sparsity distribution in the first search (with a sparsity interval of 12.5%). In the subsequent iterations (2nd, 3rd, and 4th), with sparsity intervals of 6.25%, 3.125%, and 1.5625%, respectively, the sparsity distribution is progressively refined and optimized, ultimately converging to an optimal solution.

A.5 Sparsity Distribution of Different Pruning Methods

Different pruning methods vary in the distribution of sparsity. Figure 6(a) and Figure 6(b) show the sparsity distributions of MHA and FFN of Llama-3.1-8B after 50% pruning by a series of LLM structural pruning methods, respectively.

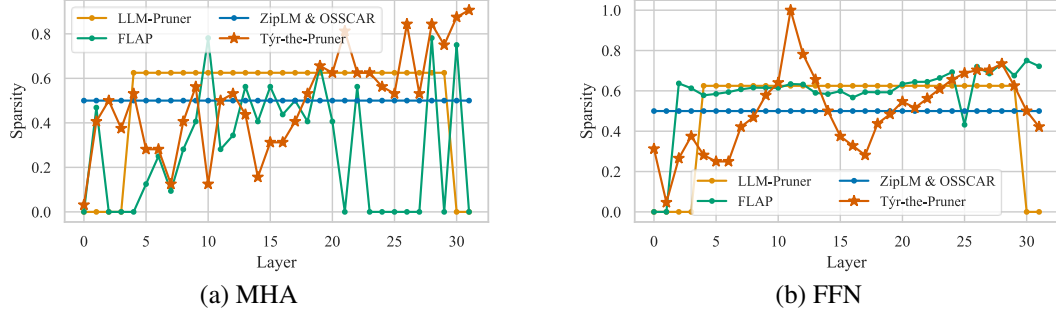


Figure 6: Sparsity distributions with different structural pruning methods.

ZipLM and OSSCAR maintain isotropic sparsity distribution. LLM-Pruner incorporates prior knowledge, recognizing that the shallow and deep layers of LLMs are more pruning-sensitive and thus preserve them while only isotropically pruning the intermediate layers. These three methods fail to account for the unique characteristics of different LLMs, leading to clear suboptimal sparsity assignments. Conversely, FLAP combines local activations and weights to assess the global sparsity distribution, resulting in non-isotropic pruning. While this method seeks a balance between local and global sparsity, it does not fully address the gap between them, making it challenging to achieve an optimal sparsity distribution.

Týr-the-Pruner’s sparsity distribution clearly differs from that of other methods. It directly searches for the optimal sparsity distribution at the global level without the local and global gaps. The resulting sparsity distribution does not adhere to prior assumptions: for instance, the 2-nd FFN layer is largely retained, while the 12-th FFN layer is entirely pruned, and there is no discernible pattern in the sparsity ratio as layers become deeper or shallower. This demonstrates that model optimization should fully account for the model’s unique characteristics.

A.6 Prune and Tune

Table 10: **Results of pruning and finetuning.** Perplexity on Wikitext2 (lower is better) and accuracy (% higher is better) serve as the comparison metrics. MMLU employed a 5-shot benchmark, while other tasks used 0-shot benchmarks. An asterisk (*) indicates a fine-tuned result. Optimal and suboptimal results are **bolded** and underlined, respectively.

Sparsity	Method	Wikitext2 ↓	Avg. Acc. ↑	Arc-C ↑	Arc-E ↑	BoolQ ↑	HellaSwag ↑	OBQA ↑	RTE ↑	WinoGrande ↑	MMLU ↑
0%	N/A	5.84	64.77	51.54	81.31	82.17	60.04	33.20	71.12	73.56	65.20
37.5%	LLM-Pruner	70.93	32.87	19.68	32.07	40.03	27.55	13.20	52.71	50.83	26.88
	LLM-Pruner*	17.97	47.11	32.51	64.18	63.09	47.79	26.00	55.23	58.56	29.53
	NutePrune*	14.31	51.33	36.77	62.92	68.78	49.45	29.20	58.12	66.93	38.49
	FLAP	21.54	43.07	23.98	52.15	64.62	36.50	23.40	55.60	58.17	30.17
	FLAP*	18.47	48.43	34.39	62.33	65.87	44.77	28.80	56.68	58.88	35.74
	Týr-the-Pruner	18.09	53.46	39.68	73.53	70.55	47.12	30.00	58.84	66.54	41.43
50%	Týr-the-Pruner*	12.65	58.22	46.93	77.02	75.75	54.99	32.60	59.57	68.82	50.06
	LLM-Pruner	288.32	31.58	19.62	28.70	37.83	26.36	13.40	52.35	49.64	24.70
	LLM-Pruner*	27.34	40.39	25.68	53.49	45.84	39.88	22.00	53.79	55.25	27.22
	NutePrune*	<u>23.55</u>	42.71	30.01	53.84	55.61	38.02	24.20	55.23	58.25	26.50
	FLAP	134.28	36.59	20.99	43.18	52.29	29.43	16.80	52.71	54.14	23.18
	FLAP*	51.29	43.01	29.18	53.32	60.83	37.15	22.00	56.68	57.14	27.77
	Týr-the-Pruner	30.89	47.79	31.83	65.36	66.64	39.99	24.80	58.12	61.80	33.76
	Týr-the-Pruner*	19.68	51.83	38.65	70.92	67.25	48.62	31.60	60.29	62.12	35.22

Structured pruning is often followed by parameter-efficient fine-tuning to restore model performance. To evaluate the benefits of our proposed method, Týr-the-Pruner, in the context of post-pruning

fine-tuning, we conducted fine-tuning experiments on the Llama-3.1-8B model. The fine-tuning employed the parameter-efficient method LoRA (rank=16) [14], and the post-pruned LLM was fine-tuned for three epochs on the Alpaca-GPT4 dataset [32].

Table 10 presents the experimental results. Týr-the-Pruner demonstrates superior performance at both 37.5% and 50% sparsity, with many of the results without fine-tuning already outperforming those fine-tuned by other methods. Furthermore, Týr-the-Pruner surpasses the state-of-the-art training-aware pruning method, NutePrune [20].

A.7 Statistical Significance Analysis

To verify the robustness of the proposed method, Týr-the-Pruner, we adjust the random seeds (the change of random seeds triggers the change of calibration samples and the change in random sparsity shift) for multiple (number of tests: $n=5$) experiments and observe the error bar (\pm standard deviation), as shown in Table 11.

From the global observation of experimental results, the proposed method performs relatively consistently in multiple randomized trials, with standard deviations within acceptable limits (< 0.21 for Wikitext2 perplexity and < 0.33 for downstream performance). From the local observation of experimental results, it can be seen that pruning yields a more stable performance for larger models or under lower sparsity ratios.

Table 11: Statistical significance analysis for Týr-the-Pruner.

Model	Sparsity	Wikitext2 ↓	BoolQ ↑	ARC-E ↑	ARC-C ↑
Llama-2-7B	25%	7.51 ± 0.07	69.45 ± 0.04	75.13 ± 0.10	42.58 ± 0.09
Llama-2-13B	25%	5.79 ± 0.00	81.35 ± 0.06	77.74 ± 0.03	44.97 ± 0.05
Llama-3.1-8B	25%	10.38 ± 0.11	76.36 ± 0.12	77.23 ± 0.09	45.48 ± 0.06
	50%	30.89 ± 0.21	66.64 ± 0.26	65.86 ± 0.33	31.83 ± 0.16

A.8 Detailed Downstream Task Results

Table 12: 0-shot acc (%) on ARC-Challenge.

Sparsity	Method	LLaMA-2		LLaMA-3.x		Mistral	
		7B	13B	2-3B	0-8B	1-8B	7B-v0.3
0%	N/A	43.43	48.46	42.32	50.43	51.54	48.81
12.5%	ShortGPT	36.18	43.86	37.80	43.94	44.20	43.43
	LaCO+	37.97	43.60	37.63	43.69	44.20	42.15
	SliceGPT	41.81	46.25	35.15	41.64	42.15	42.49
	Wanda-sp	43.34	45.05	24.06	19.28	34.04	46.16
	LLM-Pruner	38.40	44.45	31.83	38.57	37.97	40.02
	ZipLM	41.55	49.15	38.23	40.19	42.49	47.27
	OSSCAR	42.41	49.23	38.14	40.70	40.78	46.59
	FLAP	40.02	42.15	33.45	41.30	41.47	43.86
	Týr-the-Pruner	42.06	48.05	38.82	47.44	49.15	48.55
							54.35
25%	ShortGPT	32.34	37.88	30.97	26.88	27.39	33.96
	LaCO+	30.89	38.65	32.34	36.26	36.77	33.87
	SliceGPT	37.88	41.47	28.33	35.32	37.46	38.99
	Wanda-sp	38.14	20.82	18.09	16.89	19.20	37.37
	LLM-Pruner	28.24	37.63	22.35	26.11	24.77	31.66
	ZipLM	39.51	46.93	29.52	18.43	20.31	43.69
	OSSCAR	40.53	45.65	18.17	27.47	23.46	42.66
	FLAP	31.91	40.78	26.54	31.91	33.45	36.52
	Týr-the-Pruner	42.58	44.97	35.41	42.15	45.48	44.88
							48.38
37.5%	ShortGPT	28.58	31.14	25.85	26.88	27.56	29.10
	LaCO+	28.24	32.08	25.43	27.30	27.05	28.24
	SliceGPT	32.00	36.60	23.29	27.65	27.39	28.67
	Wanda-sp	27.99	21.76	20.39	20.90	19.97	20.65
	LLM-Pruner	17.58	24.40	17.49	16.89	16.98	20.90
	ZipLM	33.53	32.08	20.56	19.80	21.16	38.31
	OSSCAR	35.49	33.96	18.77	26.54	23.98	36.77
	FLAP	29.18	35.75	24.40	25.17	23.98	29.69
	Týr-the-Pruner	38.31	43.26	30.97	38.99	39.68	38.31
							42.41
50%	ShortGPT	23.44	28.16	21.84	23.29	23.56	26.19
	LaCO+	23.55	27.05	21.25	24.74	22.87	24.49
	SliceGPT	24.91	30.63	18.86	20.99	21.50	19.45
	Wanda-sp	17.58	19.54	20.73	18.60	19.54	18.00
	LLM-Pruner	18.60	19.54	19.11	17.32	19.62	18.52
	ZipLM	20.14	27.99	19.20	17.15	20.48	23.72
	OSSCAR	23.81	25.34	20.56	17.58	19.97	27.13
	FLAP	29.10	27.47	22.78	21.76	20.99	25.34
	Týr-the-Pruner	33.62	39.85	25.51	32.34	31.83	32.94
							32.59

Table 14: 0-shot acc (%) on BoolQ.

Sparsity	Method	LLaMA-2		LLaMA-3.x		Mistral	
		7B	13B	2-3B	0-8B	1-8B	7B-v0.3
0%	N/A	77.68	80.61	73.00	81.10	82.17	82.17
12.5%	ShortGPT	74.77	75.84	63.30	73.70	70.70	77.31
	LaCO+	61.13	68.90	62.72	72.78	70.06	77.19
	SliceGPT	73.12	80.67	68.99	75.75	75.57	81.19
	Wanda-sp	71.68	77.28	51.90	53.64	63.09	77.31
	LLM-Pruner	76.48	80.43	65.72	74.34	71.90	72.72
	ZipLM	69.38	82.84	65.60	75.63	77.00	82.26
	OSSCAR	69.02	83.00	68.59	74.80	79.91	81.53
	FLAP	70.98	76.21	60.06	73.49	71.87	77.49
	Týr-the-Pruner	70.67	82.78	72.32	80.12	80.24	82.11
							82.94
25%	ShortGPT	62.17	62.54	44.83	37.80	37.65	67.25
	LaCO+	50.83	58.23	70.64	63.85	59.14	75.14
	SliceGPT	68.93	79.27	65.81	72.02	67.68	75.78
	Wanda-sp	68.90	62.17	46.02	48.90	42.17	62.45
	LLM-Pruner	62.97	68.35	61.59	60.89	57.89	68.78
	ZipLM	67.19	81.31	59.20	56.02	65.08	77.16
	OSSCAR	66.42	79.48	54.28	60.06	65.66	77.13
	FLAP	65.47	68.81	64.89	68.29	67.28	65.14
	Týr-the-Pruner	69.45	81.35	67.89	76.02	76.36	79.39
							82.26
37.5%	ShortGPT	62.17	37.25	68.87	56.57	55.66	45.60
	LaCO+	62.11	62.78	63.30	48.78	45.38	63.12
	SliceGPT	63.00	71.44	42.08	50.49	46.85	65.41
	Wanda-sp	62.26	62.17	52.66	38.13	51.68	62.05
	LLM-Pruner	61.74	62.11	50.70	41.31	40.03	62.35
	ZipLM	64.89	76.79	49.76	51.56	61.47	69.91
	OSSCAR	64.65	74.25	49.54	58.01	62.26	67.37
	FLAP	63.40	65.60	61.93	62.66	64.62	62.54
	Týr-the-Pruner	68.87	80.76	66.33	70.09	70.55	70.85
							74.65
50%	ShortGPT	62.17	62.20	46.61	62.57	62.17	51.90
	LaCO+	54.83	59.51	44.40	55.32	51.41	42.66
	SliceGPT	57.16	62.26	40.76	41.74	38.56	51.13
	Wanda-sp	46.91	62.14	41.59	54.77	40.37	48.99
	LLM-Pruner	38.23	61.31	38.10	39.54	37.83	43.24
	ZipLM	43.79	64.80	44.95	54.19	57.43	62.72
	OSSCAR	61.62	62.94	56.48	53.36	61.04	60.95
	FLAP	58.50	65.14	51.25	61.65	52.29	61.47
	Týr-the-Pruner	65.54	74.46	62.26	65.63	66.64	62.17
							65.26

Table 13: 0-shot acc (%) on ARC-Easy.

Sparsity	Method	LLaMA-2		LLaMA-3.x		Mistral	
		7B	13B	2-3B	0-8B	1-8B	7B-v0.3
0%	N/A	76.30	79.46	74.49	80.05	81.31	79.67
12.5%	ShortGPT	65.87	75.55	68.10	71.17	72.18	71.51
	LaCO+	68.39	75.04	64.69	73.44	75.67	71.25
	SliceGPT	73.40	77.78	67.68	74.71	75.51	76.85
	Wanda-sp	74.62	76.43	48.95	28.70	64.44	77.61
	LLM-Pruner	72.05	77.10	62.92	70.83	72.47	73.32
	ZipLM	75.72	79.80	71.51	73.74	75.34	78.62
	OSSCAR	76.01	79.59	71.55	74.37	76.05	78.28
	FLAP	71.38	72.69	64.44	73.36	74.16	75.76
	Týr-the-Pruner	75.84	79.62	72.94	79.08	79.80	81.61
25%	ShortGPT	52.74	61.24	49.58	38.85	43.18	52.57
	LaCO+	53.03	62.47	49.41	53.41	55.47	52.23
	SliceGPT	71.80	74.92	58.67	67.80	68.60	71.46
	Wanda-sp	70.41	33.59	37.46	42.26	28.41	70.83
	LLM-Pruner	59.97	70.20	50.72	59.43	57.79	64.02
	ZipLM	74.66	78.45	61.32	27.86	26.47	75.88
	OSSCAR	74.45	77.57	27.95	53.70	40.03	75.59
	FLAP	64.23	69.23	53.96	60.31	65.95	67.22
	Týr-the-Pruner	75.13	77.74	69.40	75.63	77.23	80.13
37.5%	ShortGPT	34.25	37.75	30.39	31.23	32.83	32.87
	LaCO+	30.01	37.71	29.00	28.58	28.54	30.18
	SliceGPT	48.40	54.84	36.20	41.33	41.62	43.56
	Wanda-sp	57.03	32.37	26.94	25.72	25.00	47.90
	LLM-Pruner	38.93	54.76	31.69	32.53	32.07	47.10
	ZipLM	68.48	61.95	27.99	27.10	27.02	70.54
	OSSCAR	68.90	62.16	28.03	54.21	47.10	70.08
	FLAP	53.45	58.16	46.55	46.63	52.15	56.65
	Týr-the-Pruner	71.13	76.35	64.52	72.56	73.53	71.38
50%	ShortGPT	34.25	37.75	30.39	31.23	32.83	32.87
	LaCO+	42.16	49.34	39.36	43.97	43.92	42.73
	SliceGPT	46.16	49.84	39.29	43.29	42.10	44.24
	Wanda-sp	51.21	34.47	28.87	28.04	27.25	44.23
	LLM-Pruner	38.80	46.81	32.91	33.94	33.05	38.66
	ZipLM	51.57	55.93	33.39	32.32	30.47	51.34

Table 16: 0-shot acc (%) on OpenBookQA.

Sparsity	Method	LLaMA-2		LLaMA-3.x		Mistral		7B-v0.3	Nemo
		7B	13B	2-3B	0-8B	1-8B			
0%	N/A	31.40	35.20	31.00	34.80	33.20	33.40	36.40	
12.5%	ShortGPT	28.20	33.20	26.60	33.00	30.80	27.00	31.60	
	LaCO+	30.00	30.20	25.60	30.80	31.20	25.60	28.80	
	SliceGPT	32.00	34.00	27.20	28.60	26.60	27.20	26.40	
	Wanda-sp	31.60	32.00	15.40	13.20	22.80	28.00	28.60	
	LLM-Pruner	28.40	34.40	24.60	27.20	26.40	26.80	31.00	
	ZipLM	31.60	34.60	27.50	28.00	26.60	34.20	32.80	
	OSSCAR	31.20	35.80	27.00	25.40	26.40	32.60	31.80	
	FLAP	29.20	32.40	27.60	30.60	30.40	33.40	31.60	
25%	Týr-the-Pruner	31.20	35.80	29.20	33.40	34.60	34.20	34.80	
	ShortGPT	23.40	27.00	23.20	19.60	18.40	20.40	23.00	
	LaCO+	25.20	25.20	22.40	20.60	20.00	23.40	22.20	
	SliceGPT	25.00	30.40	23.00	24.40	22.60	23.00	23.00	
	Wanda-sp	29.20	17.80	12.40	14.20	13.40	26.60	21.20	
	LLM-Pruner	21.00	28.80	15.40	19.80	18.00	20.40	21.00	
	ZipLM	31.40	34.80	17.60	24.40	18.80	29.20	19.20	
	OSSCAR	31.40	34.20	13.00	20.20	21.60	24.40	21.00	
37.5%	FLAP	27.40	29.80	24.60	26.60	28.40	29.80	28.00	
	Týr-the-Pruner	31.60	34.20	28.20	34.00	31.80	33.40	31.80	
	ShortGPT	21.60	17.80	18.80	18.80	18.40	17.20	17.20	
	LaCO+	17.00	21.40	17.00	17.80	16.60	17.00	19.80	
	SliceGPT	19.80	27.20	17.60	17.00	15.00	17.00	17.40	
	Wanda-sp	17.60	13.40	11.80	12.60	11.80	14.80	12.60	
	LLM-Pruner	12.80	17.80	12.20	12.80	13.20	14.80	13.00	
	ZipLM	25.60	27.00	13.80	14.40	13.20	21.80	14.60	
50%	OSSCAR	25.20	26.40	14.20	15.20	14.80	21.60	17.80	
	FLAP	24.20	27.20	21.60	22.80	23.40	24.00	25.80	
	Týr-the-Pruner	31.00	32.40	26.00	29.80	30.00	26.20	29.20	

Table 18: 0-shot acc (%) on WinoGrande.

Sparsity	Method	LLaMA-2		LLaMA-3.x		Mistral		7B-v0.3	Nemo
		7B	13B	2-3B	0-8B	1-8B			
0%	N/A	69.06	72.22	69.06	73.01	73.56	73.64	73.64	
12.5%	ShortGPT	68.98	71.03	67.64	71.67	70.09	70.24	74.11	
	LaCO+	68.35	70.96	69.61	73.16	73.16	71.35	74.03	
	SliceGPT	67.32	70.48	60.54	67.17	66.61	70.64	64.01	
	Wanda-sp	67.64	70.72	52.01	51.38	58.80	66.54	62.27	
	LLM-Pruner	64.25	69.30	60.93	65.35	65.51	66.06	68.51	
	ZipLM	14.00	19.60	12.40	13.80	11.60	17.40	13.20	
	OSSCAR	17.00	20.00	11.80	11.60	10.60	16.60	14.40	
	FLAP	21.20	25.80	13.20	21.40	16.80	21.40	21.00	
25%	Týr-the-Pruner	27.20	30.40	20.40	26.60	24.80	22.80	26.20	
	ShortGPT	65.67	70.96	61.40	53.99	55.17	67.25	63.14	
	LaCO+	64.25	69.77	63.14	67.32	65.27	67.80	71.59	
	SliceGPT	65.27	70.40	57.62	62.67	59.75	61.48	58.25	
	Wanda-sp	63.69	54.30	51.78	48.78	49.57	60.62	57.06	
	LLM-Pruner	57.70	61.56	52.57	55.41	55.17	56.20	57.62	
	ZipLM	67.98	72.38	51.85	58.88	66.93	72.53	65.98	
	OSSCAR	68.11	70.56	52.72	56.91	56.75	64.33	55.41	
37.5%	FLAP	64.72	68.03	57.06	62.75	63.46	64.72	64.64	
	Týr-the-Pruner	68.51	72.06	64.01	71.11	71.11	71.11	70.01	
	ShortGPT	60.30	65.98	61.56	54.54	55.09	59.19	53.99	
	LaCO+	59.04	65.82	58.01	60.38	61.25	59.43	55.49	
	SliceGPT	46.73	65.19	55.09	54.78	53.04	55.80	54.85	
	Wanda-sp	49.49	49.57	48.38	51.30	49.49	49.33	51.38	
	LLM-Pruner	51.07	52.57	49.96	51.07	50.83	51.78	50.36	
	ZipLM	60.46	63.46	50.36	53.83	54.38	57.38	51.14	
50%	OSSCAR	61.64	63.14	50.04	55.09	54.46	57.38	53.83	
	FLAP	61.72	64.96	52.57	57.85	58.17	57.38	56.20	
	Týr-the-Pruner	66.93	72.06	60.22	66.54	66.54	64.17	65.27	
	ShortGPT	56.20	61.80	51.46	54.70	54.14	53.12	52.64	
	LaCO+	51.38	59.19	51.22	53.75	52.17	51.30	50.12	
	SliceGPT	54.62	56.99	51.30	50.99	49.88	51.38	49.33	
	Wanda-sp	49.17	50.04	51.07	47.43	51.22	49.88	48.07	
	LLM-Pruner	50.43	49.88	51.07	50.12	49.64	50.20	49.80	
25%	ZipLM	48.54	61.91	51.54	49.17	52.49	51.93	50.59	
	OSSCAR	51.54	52.80	51.70	48.86	51.14	52.49	50.43	
	FLAP	56.51	61.72	50.51	52.80	54.14	52.88	52.09	
	Týr-the-Pruner	62.12	70.09	53.28	60.30	61.80	59.43	59.04	

Table 17: 0-shot acc (%) on RTE.

Sparsity	Method	LLaMA-2		LLaMA-3.x		Mistral		7B-v0.3	Nemo
		7B	13B	2-3B	0-8B	1-8B			
0%	N/A	62.82	65.34	54.87	67.87	71.12	68.95	64.26	
12.5%	ShortGPT	55.96	63.90	55.96	57.04	62.82	70.04	57.40	
	LaCO+	63.54	58.48	57.40	68.23	70.40	65.34	64.26	
	SliceGPT	64.26	58.84	58.48	64.62	63.90	66.06	57.40	
	Wanda-sp	58.48	64.98	46.93	57.04	57.76	57.76	62.82	
	LLM-Pruner	62.82	61.73	48.38	56.68	61.01	65.34	55.60	
	ZipLM	61.37	63.18	50.18	66.06	60.65	68.23	61.37	
	OSSCAR	58.84	61.73	56.32	64.62	63.18	69.31	59.57	
	FLAP	57.76	59.21	50.54	52.35	55.96	67.51	56.68	
25%	Týr-the-Pruner	66.06	71.15	56.68	66.79	71.84	68.95	62.82	
	ShortGPT	57.76	59.57	48.38	62.82	63.90	64.98	63.54	
	LaCO+	53.79	62.45	57.04	63.90	58.12	64.26	58.12	
	SliceGPT	53.43	58.48	53.07	52.71	53.43	55.23	52.71	
	Wanda-sp	48.38	52.71	52.71	52.71	53.43	53.79	53.43	
	LLM-Pruner	56.68	50.54	52.35	53.07	53.07	55.23	53.07	
	ZipLM	55.60	68.23	55.23	50.18	51.99	68.95	53.43	
	OSSCAR	53.65	67.51	48.74	54.51	50.54	63.18	53.79	
37.5%	FLAP	53.25	67.51	48.34	51.26	55.60	53.79	55.96	
	Týr-the-Pruner	62.09	69.31	59.57	63.90	63.18	65.34	59.57	
	ShortGPT	62.09	52.35	58.48	50.54	53.79	49.82	53.79	
	LaCO+	51.26	60.65	51.62	51.62	51.62	51.26	50.54	
	SliceGPT	51.62	61.01	54.70	51.62	45.13	53.43	49.82	
	Wanda-sp	53.43	52.71	53.07	53.43	55.96	53.07	52.71	
	LLM-Pruner	53.07	52.71	52.71	52.71	52.35	52.71	53.07	
	ZipLM	52.71	52.71	53.07	52.35	52.71	52.71	51.26	
50%	OSSCAR	53.43	52.71	50.90	47.65	51.26	53.79	55.96	
	FLAP	45.49	58.48	51.62	53.07	52.71	52.71	55.23	
	Týr-the-Pruner	55.99	59.33	53.43	58.84	58.12	53.79	60.65	
	ShortGPT	37.38	48.00	36.10	34.30	34.88	59.66	50.66	
	LaCO+	43.63	53.82	39.36	35.78	59.68	55.28	62.63	
	SliceGPT	42.88	53.43	55.85	47.34</				